PHYSICAL REVIEW B **93**, 205432 (2016)

Local density of states and its mesoscopic fluctuations near the transition to a superconducting state in disordered systems

I. S. Burmistrov,[1,2] I. V. Gornyi,[3,4,5,1] and A. D. Mirlin[3,5,6,1]
[1]*L. D. Landau Institute for Theoretical Physics, Kosygina street 2, 117940 Moscow, Russia*
[2]*Moscow Institute of Physics and Technology, 141700 Moscow, Russia*
[3]*Institut für Nanotechnologie, Karlsruhe Institute of Technology, 76021 Karlsruhe, Germany*
[4]*A. F. Ioffe Physico-Technical Institute, 194021 St. Petersburg, Russia*
[5]*Institut für Theorie der kondensierten Materie, Karlsruhe Institute of Technology, 76128 Karlsruhe, Germany*
[6]*Petersburg Nuclear Physics Institute, 188300 St. Petersburg, Russia*

(Received 9 March 2016; revised manuscript received 5 May 2016; published 20 May 2016)

We develop a theory of the local density of states (LDOS) of disordered superconductors, employing the nonlinear sigma-model formalism and the renormalization-group framework. The theory takes into account the interplay of disorder and interaction couplings in all channels, treating the systems with short-range and Coulomb interactions on equal footing. We explore two-dimensional systems that would be Anderson insulators in the absence of interaction and two- or three-dimensional systems that undergo an Anderson transition in the absence of interaction. We evaluate both the average tunneling density of states and its mesoscopic fluctuations which are related to the LDOS multifractality in normal disordered systems. The obtained average LDOS shows a pronounced depletion around the Fermi energy, both in the metallic phase (i.e., above the superconducting critical temperature T_c) and in the insulating phase near the superconductor-insulator transition (SIT). The fluctuations of the LDOS are found to be particularly strong for the case of short-range interactions, especially, in the regime when T_c is enhanced by Anderson localization. On the other hand, the long-range Coulomb repulsion reduces the mesoscopic LDOS fluctuations. However, also in a model with Coulomb interaction, the fluctuations become strong when the systems approach the SIT.

DOI: 10.1103/PhysRevB.93.205432

I. INTRODUCTION

Disordered superconductors show remarkable physics governed by interplay of superconductivity and Anderson localization. In particular, in two-dimensional (2D) systems, the competition between these two phenomena leads to a direct quantum phase transition between the insulating and superconducting states: the superconductor-insulator transition (SIT) [1,2]. This is a zero-temperature transition that may be driven by varying the normal-state resistivity of a disordered film; experimentally, this is usually achieved by changing the film thickness. At a finite (but sufficiently low) temperature the insulating and superconducting phases of the film are separated by a metallic state. The physics of SIT and, more generally, of insulating, superconducting, and metallic states around SIT, has attracted a great deal of attention.

On the experimental side, two complementary approaches have been widely used to characterize the physics of disordered superconducting films under variation of temperature, film thickness, and magnetic field: (i) transport measurements and (ii) space-resolved tunneling spectroscopy. In this paper, we focus on the second one and develop a theory of local density of states (LDOS), including both its disorder-averaged value and fluctuations, as measured in space-resolved tunneling experiments.

Particularly intriguing experimental findings on tunneling spectroscopy of 2D disordered superconducting systems were provided by experiments on TiN and InO films [3–6]. In short, it was found that (i) the pronounced soft gap in the tunneling spectrum survives across the superconductor-metal transition (i.e., with increasing temperature T above T_c) and across SIT, and (ii) there are strong point-to-point fluctuations of the shape of the energy dependence of LDOS on the superconducting side of the transition (i.e., below T_c). These results have been interpreted as evidence of (i) the existence of preformed Cooper pairs leading to a "pseudogap" in the nonsuperconducting states (metallic and insulating) [3–6] and (ii) localization of some of Cooper pairs on the superconducting side of the transition, with the fraction of localized Cooper pairs increasing when the system approaches the SIT [5]. Qualitatively similar features, although considerably less pronounced, were observed in experiments on NbN films [7,8]. Finally, a recent work on MoC films [9] did not discover any sizable "pseudogap" or spatial fluctuations effects at all; the gap observed there was related to T_c by the standard formula of the Bardeen-Cooper-Schrieffer (BCS) theory.

In order to understand the experimental findings, including features that are common for different materials as well as differences between the materials, one clearly needs the corresponding theory. In numerical works by Ghosal, Randeria, and Trivedi [10,11], a solution of the Bogoliubov–de Gennes equations for a 2D model with short-range interaction was carried out. It was found that the tunneling density of states shows a hard gap across the SIT and strong spatial fluctuations. More recently, these results were corroborated by quantum Monte Carlo simulations [12]. While these results are very insightful, the numerical simulations for the inherently interacting problem are limited by relatively small system sizes. This makes it difficult to explore parametric dependencies of observables in a sufficiently broad range, especially since the problem is characterized by a hierarchy of relevant length and energy scales. Such parametric dependencies may be studied within analytical approaches, which are also expected to shed more light on underlying physical mechanisms. Feigel'man, Ioffe, Kravtsov, Yuzbashyan, and Cuevas [13,14], studied the LDOS for a 3D system in the vicinity of Anderson-localization transition within a solution of the self-consistent BCS-type equation for the case of a short-range interaction. They found that a pseudogap develops when the superconductor is built out of localized single-particle states, and that this pseudogap increases when the system approaches the SIT.

In this paper, we develop a theory of the LDOS of disordered superconductors which employs the nonlinear sigma-model (NLSM) formalism and the renormalization-group (RG) framework, and goes beyond the analysis of Refs. [13,14] in several important aspects. First, our theory takes into account mutual influence of disorder and interaction couplings in all channels. This influence leads to the renormalization that becomes strong for systems with sufficiently strong disorder (in particular those that are not too far from SIT). Second, we consider 2D systems with short-range and Coulomb interaction on equal footing. Third, we use the same formalism to explore (i) 2D systems that would be Anderson insulators in the absence of interaction and (ii) 2D or 3D systems that undergo Anderson transition in the absence of interaction. Fourth, we evaluate both the average LDOS and its mesoscopic fluctuations (which are related to the LDOS multifractality in normal disordered systems). Fifth, when calculating the average LDOS and its moments, we take into account renormalization effects originating from all interaction channels.

On the technical side, we exploit our recent works in two complementary directions: Refs. [15,16], where the phase diagram and transport characteristics of 2D disordered systems around SIT were studied by means of the NLSM renormalization group, on the one hand, and Refs. [17–19], where the LDOS multifractality was studied near Anderson metal-insulator transition (MIT) in a normal (i.e., not superconducting) system with Coulomb interaction, on the other hand. Application of a unified approach to the LDOS and its fluctuations near MIT [17–19] and in disordered superconductors (this work) turns out to be very helpful for understanding similarities and differences between the two cases. We will return to this issue in the end of the paper.

The outline of the paper is as follows. In Sec. II, we introduce the NLSM formalism and construct operators corresponding to the moments of LDOS. The anomalous dimensions of the moments of LDOS found within the two-loop approximation are presented in Sec. III. The obtained two-loop results are used in Sec. IV to analyze the scaling behavior of the disorder-averaged LDOS and of the LDOS moments for the following three cases: (i) superconducting transition in 2D system with weak short-ranged interactions; (ii) superconducting transition in 2D system with Coulomb interaction; (iii) superconducting transition in a system with weak short-ranged interactions which, in the absence of interactions, is close to the Anderson transition. Our results and conclusions are summarized in Sec. V. Several appendixes contain technical details on the one- and two-loop RG equations and their analysis.

II. FORMALISM

A. NLSM action

We start with the description of the NLSM formalism to be used for the calculation of the local density of states and its fluctuations near the transition to the superconducting state. The action of the NLSM is given as a sum of the noninteracting part S_σ [20,21] and terms $S_{\rm int}^{(\rho,\sigma,c)}$ arising from the interactions in the particle-hole singlet and triplet, and Cooper channels [22,23] (see Refs. [24,25] for review):

$$S = S_\sigma + S_{\rm int}^{(\rho)} + S_{\rm int}^{(\sigma)} + S_{\rm int}^{(c)}, \tag{1}$$

where

$$\begin{aligned}
S_\sigma &= -\frac{g}{32}\int d\boldsymbol{r}\,\mathrm{Tr}(\nabla Q)^2 + 4\pi T Z_\omega \int d\boldsymbol{r}\,\mathrm{Tr}\,\eta Q,\\
S_{\rm int}^{(\rho)} &= -\frac{\pi T}{4}\Gamma_s \sum_{\alpha,n}\sum_{r=0,3}\int d\boldsymbol{r}\,\mathrm{Tr}\big[I_n^\alpha t_{r0} Q\big]\mathrm{Tr}\big[I_{-n}^\alpha t_{r0} Q\big],\\
S_{\rm int}^{(\sigma)} &= -\frac{\pi T}{4}\Gamma_t \sum_{\alpha,n}\sum_{r=0,3}\int d\boldsymbol{r}\,\mathrm{Tr}\big[I_n^\alpha \boldsymbol{t_r} Q\big]\mathrm{Tr}\big[I_{-n}^\alpha \boldsymbol{t_r} Q\big],\\
S_{\rm int}^{(c)} &= -\frac{\pi T}{4}\Gamma_c \sum_{\alpha,n}\sum_{r=1,2}\int d\boldsymbol{r}\,\mathrm{Tr}\big[t_{r0} L_n^\alpha Q\big]\mathrm{Tr}\big[t_{r0} L_n^\alpha Q\big].
\end{aligned}$$

Here, we use notations from Ref. [16]. The Drude conductivity (including spin) in units e^2/h is denoted as g. The quantities Γ_s, Γ_t, and Γ_c are interaction parameters in the singlet particle-hole, triplet particle-hole, and singlet Cooper channels, respectively. The parameter Z_ω introduced by Finkel'stein [22] describes the renormalization of the frequency term in the action (1).

The action (1) involves the following matrices:

$$\begin{aligned}
\Lambda_{nm}^{\alpha\beta} &= \mathrm{sgn}\, n\, \delta_{nm}\delta^{\alpha\beta} t_{00}, \quad \big(I_k^\gamma\big)_{nm}^{\alpha\beta} = \delta_{n-m,k}\delta^{\alpha\beta}\delta^{\alpha\gamma} t_{00},\\
\eta_{nm}^{\alpha\beta} &= n\,\delta_{nm}\delta^{\alpha\beta} t_{00}, \quad \big(L_k^\gamma\big)_{nm}^{\alpha\beta} = \delta_{n+m,k}\delta^{\alpha\beta}\delta^{\alpha\gamma} t_{00},
\end{aligned} \tag{2}$$

where $\alpha,\beta = 1,\dots,N_r$ stand for replica indices and integer numbers n,m correspond to the Matsubara fermionic energies $\varepsilon_n = \pi T(2n+1)$ and $\varepsilon_m = \pi T(2m+1)$. The 16 4×4 matrices

$$t_{rj} = \tau_r \otimes s_j, \quad r,j = 0,1,2,3 \tag{3}$$

act in the spin (subscript j) and particle-hole (subscript r) spaces. The corresponding Pauli matrices are defined in a standard form as follows:

$$\begin{aligned}
\tau_0 = s_0 &= \begin{pmatrix} 1 & 0 \\ 0 & 1 \end{pmatrix}, \quad \tau_1 = s_1 = \begin{pmatrix} 0 & 1 \\ 1 & 0 \end{pmatrix},\\
\tau_2 = s_2 &= \begin{pmatrix} 0 & -i \\ i & 0 \end{pmatrix}, \quad \tau_3 = s_3 = \begin{pmatrix} 1 & 0 \\ 0 & -1 \end{pmatrix}.
\end{aligned} \tag{4}$$

The vector $\boldsymbol{t_r}$ combines three 4×4 matrices, $\boldsymbol{t_r} = \{t_{r1}, t_{r2}, t_{r3}\}$. The matrix field $Q(\boldsymbol{r})$ obeys the following constraints:

$$Q^2 = 1, \quad \mathrm{Tr}\, Q = 0, \quad Q^\dagger = C^T Q^T C. \tag{5}$$

The charge-conjugation matrix $C = i t_{12}$ satisfies the following relation: $C^T = -C$. The matrix Q (as well as the trace operator Tr) acts in the replica, Matsubara, spin, and particle-hole spaces.

In the case of Coulomb interaction, the parameters Γ_s and Z_ω are related to each other, $\Gamma_s = -Z_\omega$. This relation holds in the course of the renormalization [22]. This relation also reflects the symmetry of the NLSM action (1) under the spatially independent rotations of the Q matrix (so-called $\mathcal{F}$ invariance) [16,26].

B. Moments of the local density of states

As usual, the local density of states $\rho(E,\boldsymbol{r})$ is expressed via the exact single-particle Green function. Within the NLSM formalism, the disorder-averaged LDOS is determined by the operator which is linear in Q:

$$K_1(i\varepsilon_n) = \frac{\rho_0}{4}\,\mathrm{sp}\big\langle Q^{\alpha\alpha}_{nn}\big\rangle. \tag{6}$$

Here, symbol sp denotes the trace in spin and particle-hole spaces only. The index α denotes a fixed replica and $\langle\dots\rangle$ denotes the averaging with the NLSM action (1). The density of states at energy of the order of inverse elastic scattering time $1/\tau$ is denoted by ρ_0. We remind a reader that $1/\tau$ plays a role of the high-energy (ultraviolet) cutoff of the NLSM theory. The disorder-averaged LDOS $\langle\rho(E,\boldsymbol{r})\rangle$ can be obtained after the analytic continuation of $K_1(i\varepsilon_n)$ to the real energies $i\varepsilon_n \to E + i0^+$.

Next, let us introduce the irreducible two-point correlation function

$$\begin{aligned} K_2(E,\boldsymbol{r};E',\boldsymbol{r}') &= \langle\langle\rho(E,\boldsymbol{r})\cdot\rho(E',\boldsymbol{r}')\rangle\rangle \\ &= \langle\rho(E,\boldsymbol{r})\rho(E',\boldsymbol{r}')\rangle - \langle\rho(E,\boldsymbol{r})\rangle\langle\rho(E',\boldsymbol{r}')\rangle, \end{aligned} \tag{7}$$

which allows us to find the second moment of the LDOS. In the NLSM approach, the correlator K_2 at coinciding spatial points is related to the following bilinear in Q operator:

$$\begin{aligned} P_2^{\alpha_1\alpha_2}(i\varepsilon_n,i\varepsilon_m) &= \big\langle\!\big\langle \mathrm{sp}Q^{\alpha_1\alpha_1}_{nn}(\boldsymbol{r})\cdot \mathrm{sp}Q^{\alpha_2\alpha_2}_{mm}(\boldsymbol{r})\big\rangle\!\big\rangle \\ &\quad - 2\big\langle \mathrm{sp}\big[Q^{\alpha_1\alpha_2}_{nm}(\boldsymbol{r})Q^{\alpha_2\alpha_1}_{mn}(\boldsymbol{r})\big]\big\rangle, \quad \alpha_1\neq\alpha_2. \end{aligned} \tag{8}$$

The correlation function $K_2(E,\boldsymbol{r};E',\boldsymbol{r})$ defined for real energies can be obtained from the following Matsubara counterpart:

$$K_2 = \frac{\rho_0^2}{32}\mathrm{Re}\big[P_2^{\alpha_1\alpha_2}\big(i\varepsilon_{n_1},i\varepsilon_{n_3}\big) - P_2^{\alpha_1\alpha_2}\big(i\varepsilon_{n_1},i\varepsilon_{n_2}\big)\big] \tag{9}$$

after analytic continuation: $\varepsilon_{n_1}\to E+i0^+$, $\varepsilon_{n_3}\to E'+i0^+$, and $\varepsilon_{n_2}\to E'-i0^+$. We use the convention that $n_1,n_3,n_5,\dots \geq 0$ and $n_2,n_4,n_6,\dots < 0$.

The following comments are in order here:

(i) The condition that replica indices α_1 and α_2 are nonequal in Eq. (9) stems from the fact that the two-point correlation function K_2 measures *mesoscopic fluctuations* of the LDOS. This forbids interaction lines between two fermionic loops corresponding to the LDOS in the diagrammatic approach.

(ii) The bilinear-in-Q operator (9) is an eigenoperator of the RG (or, equivalently, an exact scaling operator), i.e., it exhibits pure power scaling, without admixture of subleading power-law contributions. Below we will explicitly prove this statement by means of two-loop calculation.

(iii) Disorder-averaged higher moments of the LDOS can be expressed in terms of higher-order irreducible correlation functions of the Q field similarly to Eq. (9). Explicit examples of operators corresponding to the third and fourth moments of the LDOS can be found in Ref. [19]. The corresponding operators are also eigenoperators of the renormalization group.

III. RENORMALIZATION GROUP FOR LDOS

In this section, we outline the RG formalism in the context of the calculation of the moments of the distribution of the local DOS as derived from the NLSM.

A. Perturbative expansion

To resolve the nonlinear constraint (5) we adopt the square-root parametrization

$$Q = W + \Lambda\sqrt{1-W^2}\,, \quad W = \begin{pmatrix} 0 & w \\ \bar{w} & 0 \end{pmatrix}. \tag{10}$$

We use the following notations: $W_{n_1n_2} = w_{n_1n_2}$ and $W_{n_2n_1} = \bar{w}_{n_2n_1}$ with $n_1 \geq 0$ and $n_2 < 0$. As a consequence of the charge-conjugation constraint (5), the blocks w and $\bar{w}$ obey the following relations:

$$\bar{w} = -Cw^TC, \quad w = -Cw^*C. \tag{11}$$

These relations imply that elements $(w^{\alpha\beta}_{n_1n_2})_{rj}$ in the expansion $w^{\alpha\beta}_{n_1n_2} = \sum_{rj}(w^{\alpha\beta}_{n_1n_2})_{rj}t_{rj}$ are real or purely imaginary. The perturbative (in $1/g$) analysis of the NLSM action (1) is performed by expanding the action in powers of W.

From the expansion the NLSM action (1) to the second order in W, we find the bare propagators (see Ref. [25]). The propagators in the particle-hole channel (diffusons) read as ($r = 0,3$ and $j = 0,1,2,3$)

$$\begin{aligned} &\big\langle[w_{rj}(\boldsymbol{p})]^{\alpha_1\beta_1}_{n_1n_2}[\bar{w}_{rj}(-\boldsymbol{p})]^{\beta_2\alpha_2}_{n_4n_3}\big\rangle \\ &\quad = \frac{2}{g}\delta^{\alpha_1\alpha_2}\delta^{\beta_1\beta_2}\delta_{n_{12},n_{34}}\mathcal{D}_p\big(i\Omega^{\varepsilon}_{12}\big) \\ &\quad\quad \times\left[\delta_{n_1n_3} - \frac{32\pi T\Gamma_j}{g}\delta^{\alpha_1\beta_1}\mathcal{D}^{(j)}_p\big(i\Omega^{\varepsilon}_{12}\big)\right], \end{aligned} \tag{12}$$

where $n_{12} = n_1 - n_2$ and $\Omega^{\varepsilon}_{12} = \varepsilon_{n_1} - \varepsilon_{n_2}$. The standard diffusive propagator is given by

$$\mathcal{D}_p^{-1}(i\omega_n) = p^2 + 16Z_\omega|\omega_n|/g, \tag{13}$$

with $\omega_n = 2\pi Tn$. The diffusons renormalized by interaction in the particle-hole channels read as

$$\big[\mathcal{D}^{(j)}_p(i\omega_n)\big]^{-1} = p^2 + 16(Z_\omega+\Gamma_j)|\omega_n|/g. \tag{14}$$

The propagators in the particle-particle channel (cooperons) can be written as ($r = 1,2$ and $j = 0,1,2,3$)

$$\begin{aligned} &\big\langle[w_{rj}(\boldsymbol{q})]^{\alpha_1\beta_1}_{n_1n_2}[\bar{w}_{rj}(-\boldsymbol{q})]^{\beta_2\alpha_2}_{n_4n_3}\big\rangle \\ &\quad = \frac{2}{g}\delta^{\alpha_1\alpha_2}\delta^{\beta_1\beta_2}\delta_{n_{14},n_{32}}\mathcal{C}_q\big(i\Omega^{\varepsilon}_{12}\big) \\ &\quad\quad \times\left[\delta_{n_1n_3} - \frac{64\pi TZ_\omega}{g}\delta^{\alpha_1\beta_1}\delta_{j0}\mathcal{C}_q\big(i\Omega^{\varepsilon}_{34}\big)\mathcal{L}_q(i\mathcal{E}_{12})\right], \end{aligned} \tag{15}$$

where $\mathcal{E}_{12} = \varepsilon_{n_1} + \varepsilon_{n_2}$ and $\mathcal{C}_q(i\omega_n) \equiv \mathcal{D}_q(i\omega_n)$. The propagator $\mathcal{L}$ stands for the standard superconducting-fluctuation propagator:

$$\mathcal{L}_q^{-1}(i\omega_n) = \gamma_c^{-1} + \ln\frac{\Lambda_U}{4\pi T} - \psi\left(\frac{Dq^2+|\omega_n|}{4\pi T}+\frac{1}{2}\right) + \psi\left(\frac{1}{2}\right). \tag{16}$$

Here, we have introduced $\gamma_c = \Gamma_c/Z_\omega$. The quantity $D = g/(16Z_\omega)$ is the diffusion coefficient, $\Lambda_U \sim 1/\tau$ is the ultraviolet energy scale, and $\psi(z)$ denotes the digamma function. We note that the fluctuation propagator (16) is written under the assumption that the infrared energy scale of the theory is determined by temperature.

For the purpose of regularization in the infrared, we add the extra term

$$S \to S + \frac{gh^2}{8}\int d\boldsymbol{r}\,\mathrm{Tr}\Lambda Q \tag{17}$$

to the NLSM action (1). The presence of this term in the action results, in particular, in the substitution of p^2+h^2 for p^2 in the propagators (13), (14), and (16).

B. Disorder-averaged LDOS

For the sake of completeness, and in order to set notations, we remind then the reader the result of one-loop renormalization of the disorder-averaged LDOS. Expanding the matrix Q to the second order in W, we derive from Eq. (6) the following expression:

$$\frac{K_1(i\varepsilon_{n_1})}{\rho_0} = 1 - \frac{1}{8}\mathrm{sp}\sum_{n_2,\beta}\langle w^{\alpha\beta}_{n_1n_2}(\boldsymbol{r})\bar{w}^{\beta\alpha}_{n_2n_1}(\boldsymbol{r})\rangle. \tag{18}$$

Next, using Eqs. (12) and (15), we find

$$\frac{\rho(i\varepsilon_{n_1})}{\rho_0} = 1 + \frac{64\pi T}{g^2}\int_q\sum_{\omega_n>\varepsilon_{n_1}}\sum_{j=0}^{3}\Gamma_j\mathcal{D}_q(i\omega_n)\mathcal{D}_q^{(j)}(i\omega_n) + \frac{128\pi T Z_\omega}{g^2}\int_q\sum_{\omega_n<\varepsilon_{n_1}}\mathcal{C}_q^2(2i\varepsilon_{n_1}-i\omega_n)\mathcal{L}_q(i\omega_n). \tag{19}$$

Finally, performing the analytic continuation to real frequencies $i\varepsilon_{n_1}\to E+i0^+$, we obtain that the disorder-averaged LDOS can be written as

$$\langle\rho(E)\rangle = \rho_0[Z(E)]^{1/2}, \tag{20}$$

where the renormalization factor $Z(E)$ is given by (see Refs. [27,28] for a review)

$$Z(E) = 1 + \frac{32}{g^2}\mathrm{Im}\sum_{j=0}^{3}\Gamma_j\int_{q,\omega}\mathcal{F}_{\omega-E}\mathcal{D}_q^R(\omega)\mathcal{D}_q^{(j)R}(\omega) + \frac{64Z_\omega}{g^2}\mathrm{Im}\int_{q,\omega}\mathcal{C}_q^{R2}(2E-\omega) \times\left[\mathcal{L}_q^K(\omega)+\mathcal{F}_{E-\omega}\mathcal{L}_q^R(\omega)\right]. \tag{21}$$

Here, $\mathcal{D}_q^R(\omega)$, $\mathcal{C}_q^R(\omega)$, $\mathcal{D}_q^{(j)R}(\omega)$, and $\mathcal{L}_q^R(\omega)$ are retarded propagators obtained from the corresponding Matsubara propagators. The Keldysh part of the fluctuation propagator $\mathcal{L}_q^K(\omega)$ is related to the retarded one via the bosonic distribution function $\mathcal{B}_\omega = \coth(\omega/2T)$ as follows: $\mathcal{L}_q^K(\omega) = 2i\mathcal{B}_\omega\mathrm{Im}\mathcal{L}_q^R(\omega)$. The fermionic distribution function is denoted as $\mathcal{F}_\omega = \tanh(\omega/2T)$. We adopt the following shorthand notation:

$$\int_{q,\omega} \equiv \int\frac{d^d\boldsymbol{q}}{(2\pi)^d}\int_{-\infty}^{\infty}d\omega. \tag{22}$$

We note that the definition (20) of Z coincides with the definition of the field renormalization constant in Ref. [25] and the wave-function renormalization constant in Ref. [29]. We stress that Z differs from the Finkel'stein's frequency renormalization factor Z_ω and should not be confused with the latter.

To derive the RG equation for Z, we set temperature T and energy E to zero, neglect frequency and momentum dependence of the fluctuation propagator, and study the dependence of Z on the infrared regulator h^2. Then, in $d=2+\epsilon$ dimensions we obtain

$$Z = 1 - [\ln(1+\gamma_s)+3\ln(1+\gamma_t)+2\gamma_c]\frac{h^\epsilon t}{\epsilon} + O(\epsilon). \tag{23}$$

Here, $\gamma_{s,t} = \Gamma_{s,t}/Z_\omega$ are dimensionless interaction amplitudes and $t = 8\Omega_d/g$ denotes dimensionless resistivity, with $\Omega_d = S_d/[2(2\pi)^d]$ and $S_d = 2\pi^{d/2}/\Gamma(d/2)$ being the area of a d-dimensional sphere. As usual, Eq. (23) determines the anomalous dimension ζ of the disorder-averaged LDOS. Using the minimal subtraction scheme (see, e.g., Ref. [30]), we obtain in the one-loop approximation [23,29,31]

$$-\frac{d\ln Z}{dy} = 2\zeta = -[\ln(1+\gamma_s)+3\ln(1+\gamma_t)+2\gamma_c]t + O(t^2), \tag{24}$$

where $y=\ln 1/h$ is the running RG length scale. We note that γ_c in Eq. (24) coincides with the fluctuation propagator at zero frequency and momentum as one can see from Eq. (16). A more accurate treatment of the momentum and frequency dependence of the fluctuation propagator in Eq. (21) (see Appendix A of Ref. [16]) results in exactly the same RG equation as Eq. (24).

Thus, this one-loop RG equation is formally exact in all three interaction couplings γ_s, γ_t, and γ_c. In the case of fully broken spin-rotational symmetry, Eq. (24) holds with the contribution $3\ln(1+\gamma_t)$ of the triplet particle-hole channel in the right-hand side being omitted.

C. Second moment of the LDOS

Now, we consider the renormalization of the second moment of the LDOS. We restrict our consideration by one- and two-loop orders in t.

1. One-loop results

In the one-loop approximation, one obtains

$$\left[P_2^{\alpha_1\alpha_2}\right]^{(1)}(i\varepsilon_{n_1},i\varepsilon_{n_3}) = 0 \tag{25}$$

and

$$\left[P_2^{\alpha_1\alpha_2}\right]^{(1)}(i\varepsilon_{n_1},i\varepsilon_{n_2}) = -2\mathrm{sp}\langle w^{\alpha_1\alpha_2}_{n_1n_2}(\boldsymbol{r})\bar{w}^{\alpha_2\alpha_1}_{n_2n_1}(\boldsymbol{r})\rangle = -\frac{128}{g}\int_q\left[\mathcal{D}_q(i\Omega^\varepsilon_{12})+\mathcal{C}_q(i\Omega^\varepsilon_{12})\right]. \tag{26}$$

Hence, we find

$$K_2^{(1)}(E,\boldsymbol{r};E',\boldsymbol{r}) = \rho_0^2\frac{4}{g}\mathrm{Re}\int_q\left[\mathcal{D}^R_q(\Omega)+\mathcal{C}^R_q(\Omega)\right], \tag{27}$$

where $\Omega = E - E'$. Setting $\Omega = 0$ and using h^2 as the infrared regulator, we get

$$K_2^{(1)} = -\rho_0^2\frac{2h^\epsilon t}{\epsilon} + O(\epsilon). \tag{28}$$

2. *Two-loop results*

Details of the calculation of the two-loop contribution to the correlation function K_2 are presented in Appendix A. Using Eqs. (A4) and (A11), we find the following two-loop contribution to the irreducible two-point correlation function:

$$K_2^{(2)} = \rho_0^2\frac{t^2h^{2\epsilon}}{\epsilon^2}\Bigg\{1+2\left(1+\frac{\epsilon}{2}\right)+(3+\epsilon)\gamma_c+\sum_{j=0}^{3}\Big[f(\gamma_j) + 2\ln(1+\gamma_j)+\frac{\epsilon}{2}[\ln(1+\gamma_j)+2f(\gamma_j)-c(\gamma_j)]\Big]\Bigg\}. \tag{29}$$

Here, we define the functions

$$f(\gamma) = 1-(1+1/\gamma)\ln(1+\gamma) \tag{30}$$

and

$$c(\gamma) = 2+\frac{2+\gamma}{\gamma}\mathrm{li}_2(-\gamma)+\frac{1+\gamma}{2\gamma}\ln^2(1+\gamma), \tag{31}$$

where $\mathrm{li}_2(x) = \sum_{k=1}^\infty x^k/k^2$ denotes the polylogarithm.

3. *Anomalous dimension of the second moment of LDOS*

Above, we have derived the dependence of K_2 on the momentum scale h within the two-loop approximation. However, h itself acquires renormalization [32]. The renormalized momentum scale h' is defined as follows:

$$g'h'^2\mathrm{Tr}\Lambda^2 = gh^2\langle\mathrm{Tr}\Lambda Q\rangle, \tag{32}$$

where g' denotes the renormalized conductivity at the momentum scale h'. As a consequence of Eq. (32), h' satisfies the following relation: $g'h'^2 = gh^2Z^{1/2}$. Using Eq. (23) and the one-loop result for the conductivity [22,29,33,34]

$$g' = g\left[1+\frac{a_1t\,h^\epsilon}{\epsilon}+O(\epsilon)\right], \quad a_1 = 1+\sum_{j=0}^{3}f(\gamma_j)-\gamma_c, \tag{33}$$

we find

$$h' = h\left\{1-\frac{t\,h^\epsilon}{2\epsilon}\left[1+\sum_{j=0}^{3}\left[f(\gamma_j)+\frac{1}{2}\ln(1+\gamma_j)\right]\right]\right\}. \tag{34}$$

We note that within the one-loop approximation, there is no contribution to Eq. (34) due to interaction in the Cooper channel.

By using Eqs. (28), (29), and (34), we can rewrite the second moment of the LDOS in terms of the renormalized momentum scale h' and the renormalization factor Z as follows:

$$\langle\rho^2\rangle = Z\rho_0^2+K_2 = \rho_0^2Zm_2', \tag{35}$$

where

$$m_2' = m_2\left[1+\frac{b_1^{(2)}t\,h'^\epsilon}{\epsilon}+\frac{t^2h'^{2\epsilon}}{\epsilon^2}\left(b_2^{(2)}+\epsilon b_3^{(2)}\right)\right]. \tag{36}$$

Here, we omit the terms that are finite in the limit $\epsilon\to 0$. The bare value of m_2' is unity, $m_2 = 1$, and

$$b_1^{(2)} = -2, \quad b_2^{(2)} = 3+\sum_{j=0}^{3}f(\gamma_j)-\gamma_c, \quad b_3^{(2)} = -\frac{1}{2}\sum_{j=0}^{3}c(\gamma_j)+\gamma_c. \tag{37}$$

Next, we introduce a dimensionless quantity $\bar{t} = t'h'^\epsilon$. With the help of Eqs. (33) and (36), we express t, γ_j, and m_2 as follows:

$$t = (h')^{-\epsilon}\bar{t}Z_t(\bar{t},\gamma_s',\gamma_t'), \quad \gamma_j = \gamma_j'Z_j(\bar{t},\gamma_s',\gamma_t'), \quad m_2 = m_2'Z_{m_2}(\bar{t},\gamma_s',\gamma_t'). \tag{38}$$

The interaction parameters γ_j are renormalized at the one-loop level [22]. However, this does not affect the two-loop result for the anomalous dimension of m_2' since $b_1^{(2)}$ is independent of γ_j. To the lowest orders in $\bar{t}$, the renormalization parameters become

$$Z_t = 1+\frac{a_1}{\epsilon}\bar{t} \tag{39}$$

and

$$Z_{m_2}^{-1} = 1+\frac{b_1^{(2)}}{\epsilon}\bar{t}+\frac{\bar{t}^2}{\epsilon^2}\left[b_2^{(2)}+b_1^{(2)}a_1+\epsilon b_3^{(2)}\right]. \tag{40}$$

The anomalous dimension of m_2' is derived from standard conditions that m_2 (as well as t and γ_j) does not depend on the momentum scale h'. In this way, we obtain the following two-loop result for the anomalous dimension $\zeta_2(t,\gamma_s,\gamma_t,\gamma_c)$ of m_2':

$$-\frac{d\ln m_2}{dy} = \zeta_2 = -2t-[c(\gamma_s)+3c(\gamma_t)-2\gamma_c]t^2+O(t^3). \tag{41}$$

Here, we omit "prime" and "bar" signs for brevity. We remind the reader that the function $c(\gamma)$ is defined in Eq. (30). We note that $c(0) = 0$ as it is known for free electrons [20]. In the case of Coulomb interaction, one has $c(-1) = 2-\pi^2/6\approx 0.36$. The interaction affects the anomalous dimension at the two-loop order only.

We emphasize that coefficients a_1, $b_1^{(2)}$, and $b_2^{(2)}$ satisfy the relation

$$b_2^{(2)} = b_1^{(2)}\left(b_1^{(2)}-a_1\right)/2. \tag{42}$$

This guarantees the absence in Eq. (41) of terms divergent in the limit $\epsilon \to 0$, i.e., the renormalizability of m_2. In addition, this relation proves that the operator corresponding to K_2 is the RG eigenoperator. Indeed, if the operator corresponding to K_2 is the linear combination of several eigenoperators, the relation (42) would imply nonlinear system of equations which has no nontrivial solutions in general.

Combining the above results, the second moment of the LDOS can be written as

$$\langle \rho^2 \rangle = \langle \rho \rangle^2 m_2. \tag{43}$$

The scaling behavior of $\langle \rho \rangle$ and m_2 is governed by the anomalous dimensions (24) and (41), respectively.

D. The qth moment of the LDOS

In this section, we generalize the results obtained in the previous section for the qth moment of the LDOS. The important observation is that the irreducible qth moment of the LDOS, $K_q = \langle (\rho - \langle \rho \rangle)^q \rangle$, involves connected contributions from averages of the number q of matrices Q. Therefore, K_q has no one- and two-loop contributions for $q \geq 5$. Consequently, as in the case of noninteracting electrons [35–37], the anomalous dimension for the qth moment of the LDOS becomes proportional to the factor $q(1-q)$ within one- and two-loop approximations (see details in Ref. [19]). Thus, we find

$$\langle \rho^q \rangle = \langle \rho \rangle^q m_q, \tag{44}$$

where the behavior of m_q is determined by the following RG equation:

$$-\frac{d \ln m_q}{dy} = \zeta_q = \frac{q(1-q)}{2}\{2t + [c(\gamma_s) + 3c(\gamma_t) - 2\gamma_c]t^2\}. \tag{45}$$

Here, the function $c(\gamma)$ is defined in Eq. (30). We note that for the special cases $q = 3$ and 4, one can demonstrate that Eq. (45) holds as well (see Appendix C of Ref. [19]).

As we have already mentioned above, the two-loop contributions to $[P_2^{\alpha_1\alpha_2}]^{RA}$ can be interpreted as the renormalization of diffusions and cooperons involved in the one-loop term $[P_1^{\alpha_1\alpha_2}]^{RA}$ (see Appendix B). Therefore, within the two-loop approximation, the corrections due to fluctuating Cooper pairs to m_q comes from the term $[P_1^{\alpha_1\alpha_2}]^{RR}$ only. In the one-loop approximation, the fluctuation corrections to the qth moment of the LDOS are fully determined by those in the average LDOS via the factor $\langle \rho \rangle^q$.

In the absence of spin-rotational symmetry, the anomalous dimension ζ_q can be obtained from Eq. (45) as follows: (i) one omits the contribution $3c(\gamma_t)$ of the triplet particle-hole channel and (ii) one multiples the right-hand side of Eq. (45) by the factor $\frac{1}{4}$ (see Ref. [19]). Thus, in the case of broken spin-rotational symmetry, Eq. (45) takes the following form:

$$-\frac{d \ln m_q}{dy} = \zeta_q = \frac{q(1-q)}{2}\left\{\frac{t}{2} + \left[c(\gamma_s) - 2\gamma_c\right]\frac{t^2}{4}\right\}. \tag{46}$$

We mention that Eqs. (45) and (46) imply the normal distribution for the logarithm of the local density of states similar to the noninteracting case (see Refs. [38,39] for a review).

IV. SCALING ANALYSIS

A. Weak coupling RG equations in 2D

Recently [16], the full set of one-loop RG equations describing the renormalization of resistivity and interactions has been derived by means of the background field renormalization of the NLSM (1):

$$\frac{dt}{dy} = t^2\left[\frac{\mathcal{N}-1}{2} + f(\gamma_s) + \mathcal{N} f(\gamma_t) - \gamma_c\right], \tag{47}$$

$$\frac{d\gamma_s}{dy} = -\frac{t}{2}(1+\gamma_s)\left(\gamma_s + \mathcal{N}\gamma_t + 2\gamma_c + 4\gamma_c^2\right), \tag{48}$$

$$\frac{d\gamma_t}{dy} = -\frac{t}{2}(1+\gamma_t)\left[\gamma_s - (\mathcal{N}-2)\gamma_t - 2\gamma_c - 4\gamma_c\gamma_t + 4\gamma_c^2\right], \tag{49}$$

$$\frac{d\gamma_c}{dy} = -2\gamma_c^2 - \frac{t}{2}\big[(1+\gamma_c)(\gamma_s - \mathcal{N}\gamma_t) - 2\gamma_c^2 + 4\gamma_c^3 + 2\mathcal{N}\gamma_c(\gamma_t - \ln(1+\gamma_t))\big], \tag{50}$$

$$\frac{d \ln Z_\omega}{dy} = \frac{t}{2}\left(\gamma_s + \mathcal{N}\gamma_t + 2\gamma_c + 4\gamma_c^2\right). \tag{51}$$

Here, $\mathcal{N}$ stands for the number of triplet diffusive modes. In the case of preserved spin-rotational symmetry, all three triplet diffusons contribute to the RG equations $\mathcal{N} = 3$. If spin-rotational symmetry is broken, all triplet modes are suppressed at long length scales $\mathcal{N} = 0$. In addition, in this case the RG equation for γ_t should be ignored.

The above RG equations are derived in the lowest order in $t \ll 1$. Extending the previous result [23], in this order they contain *all* contributions due to the interaction in the Cooper channel γ_c. Comparison of the disorder-independent and disorder-induced terms in the right-hand side of Eq. (50) demonstrates that one-loop RG equations can be used towards the superconducting instability up to the length scale L_X at which $|\gamma_c(L_X)| t(L_X) \sim 1$ [16]. We note that a similar conclusion follows from comparison of one and two-loop contributions in Eqs. (45) and (46).

B. Weak short-ranged interactions in 2D

We start our analysis of the fluctuations of LDOS with the case of weak short-ranged interactions $|\gamma_{s,t,c}| \ll 1$ in two dimensions. The phase diagram and transport properties for this case have been discussed in details in Refs. [15,16]. The existence of a large region of the superconducting phase with transition temperature higher than standard expression of BCS theory has been predicted.

For the sake of convenience, we briefly remind the reader the main steps of analysis of Ref. [15]. Let us focus on the case of preserved spin-rotational symmetry. For $|\gamma_{s,t,c}| \ll 1$, the set of RG equations (47)–(50) can be simplified to

$$dt/dy = t^2, \tag{52}$$

$$\frac{d}{dy}\begin{pmatrix}\gamma_s\\ \gamma_t\\ \gamma_c\end{pmatrix} = -\frac{t}{2}\begin{pmatrix}1 & 3 & 2\\ 1 & -1 & -2\\ 1 & -3 & 0\end{pmatrix}\begin{pmatrix}\gamma_s\\ \gamma_t\\ \gamma_c\end{pmatrix} - \begin{pmatrix}0\\ 0\\ 2\gamma_c^2\end{pmatrix}. \tag{53}$$

Equation (52) yields usual weak localization behavior:

$$t^{-1}(y) = t_0^{-1} - y. \quad (54)$$

Here, $t_0 \ll 1$ denotes the bare value of resistance. In the absence of interactions, Eq. (54) suggests that a strong Anderson insulator emerges at the scale $y_I = t_0^{-1}$. In the case of not too weak interactions (or sufficiently weak disorder), $t_0 \ll |\gamma_{s,0}|,|\gamma_{t,0}|,|\gamma_{c,0}|$, Eq. (53) reduces to the standard RG equation for the BCS instability in the clean case. Then, the superconducting transition occurs at the scale of the order of $y_{\rm BCS} = 1/(2|\gamma_{c,0}|)$.

For the case of disorder which is strong compared to the interaction $t_0 \gg |\gamma_{s,0}|,|\gamma_{t,0}|,|\gamma_{c,0}|$, the renormalization proceeds in two steps. At the first step, we can neglect the $-2\gamma_c^2$ term. This brings us to a linear system of equations. The corresponding 3×3 matrix has two eigenvalues

$$\lambda = 2t, \quad \lambda' = -t, \quad (55)$$

where λ' is doubly degenerate. We emphasize that the eigenvalue λ coincides with the one-loop result for ζ_2. This occurs since the interactions in the NLSM action (1) are described by the operators bilinear in Q. Thus, three couplings tend to the eigenvector $\{-1,1,1\}$ corresponding to the positive eigenvalue λ. This eigenvector parametrizes the so-called BCS line

$$-\gamma_s = \gamma_t = \gamma_c \equiv \gamma. \quad (56)$$

It is this relation between the couplings that one obtains starting from a standard BCS Hamiltonian with the attraction only. Projecting Eqs. (53) onto the BCS line, we get

$$d\gamma/dy = 2t\gamma - 2\gamma^2/3. \quad (57)$$

We note that the RG flow in directions perpendicular to the eigenvector $\{-1,1,1\}$ does not affect the results in any essential way (see Ref. [15] for details).

We are interested in the case when the dominant bare interaction is the Cooper attraction $\gamma_{c,0} < 0$ such that the initial value $\gamma_0 = (-\gamma_{s,0} + 3\gamma_{t,0} + 2\gamma_{c,0})/6 < 0$. Equation (57) describes two distinct scenarios. For $|\gamma_0| \ll t_0^2$, the resistance t becomes of order unity when $|\gamma|$ is still small. This means that, with further increase of the length scale, the system flows toward a strong Anderson insulator.

In the opposite case $|\gamma_0| \gg t_0^2$, $|\gamma|$ increases under the RG transformation due to the first term in the right-hand side of Eq. (57). The attractive interaction overtakes t and reaches unity at the scale $y_c \approx t_0^{-1}[1 - 2|\gamma_0|/(3t_0)]$. We note that

$$t(y_c) \equiv t_c = 3t_0^2/(2|\gamma_0|) \ll 1, \quad (58)$$

i.e., strong attraction is arisen in the region of good metal. In this situation, we expect that with further increase of the length scale, the RG flow develops a superconducting instability (due to standard BCS-type mechanism). The temperature T_c of this superconducting transition can be estimated as

$$T_c \sim \frac{1}{\tau} e^{-2y_c} \sim \frac{1}{\tau} \exp\left(-\frac{2}{t_0} + \frac{2}{t_c}\right). \quad (59)$$

In the considered regime of sufficiently strong disorder, $t_0 \gg |\gamma_{s,0}|,|\gamma_{t,0}|,|\gamma_{c,0}|$, the temperature given by Eq. (59) is much higher than the clean BCS value

$$T_c^{\rm BCS} \sim \tau^{-1} e^{-2y_{\rm BCS}} \sim \tau^{-1} e^{-1/|\gamma_{c,0}|}. \quad (60)$$

When t_0 becomes smaller than $|\gamma_0|$, Eq. (59) crosses over into Eq. (60). Therefore, T_c shows a nonmonotonous dependence on the disorder strength and gets strongly enhanced in the intermediate range of resistivity $|\gamma_0| \ll t_0 \ll \sqrt{|\gamma_0|}$. For a given interaction strength $\gamma_0 = (-\gamma_{s,0} + 3\gamma_{t,0} + 2\gamma_{c,0})/6 < 0$, the superconducting critical temperature T_c is the largest when the system approaches the superconductor-insulator transition. The latter takes place at $t_c \sim 1$, i.e., $t_0 \sim \sqrt{|\gamma_0|}$. It is worth noting that at the superconductor-insulator transition the critical temperature on the superconducting side is given by $T_c \sim \delta_\xi = \tau^{-1}\xi^{-2}$, where $\xi \sim l\exp(-2/t_0)$ is the localization length defined such as $t(\xi) \sim 1$.

The above analysis [15] for $|\gamma_{s,t,c}| \ll 1$ was extended in Ref. [16] to the case of strong interaction couplings. The numerical integration of the full RG equations (47)–(50) provided the phase diagram of the SIT. In particular, it was found that, when the system is initially close to the BCS line, the enhancement of T_c occurs for $|\gamma_{c,0}| \lesssim 0.2$.

Now, let us return to the LDOS and consider RG equations (24) and (45) in the intermediate range of parameters $|\gamma_0| \ll t_0 \ll \sqrt{|\gamma_0|}$. For temperatures $T \gg T_c$, the behavior of the disorder-averaged LDOS is fully determined by Eq. (24) expanded to the lowest order in interaction parameters. After projection to the BCS line (56), we find from Eq. (24)

$$\frac{d\ln Z}{dy} = 4\gamma t. \quad (61)$$

Solving this equation together with Eqs. (52) and (57), we obtain

$$\frac{\langle\rho(E)\rangle}{\rho_0} = 1 + \gamma_0\left(\frac{t^2}{t_0^2} - 1\right), \quad (62)$$

where t should be taken at the scale $\min\{L_T,L_E\}$. Since we consider $T \gg T_c$, the resistivity $t(\min\{L_T,L_E\}) \ll t_c$. This allowed us to neglect the second term in the right-hand side of Eq. (57). As one can see from (62), there is a weak suppression of the averaged LDOS for $t_0 \ll \sqrt{|\gamma_0|}$. On the other hand, Eq. (45) results in the following dependence of m_q on t:

$$m_q = (t/t_0)^{q(q-1)}. \quad (63)$$

Here, we omit the two-loop contribution since within our approximation it is always much smaller than the one-loop one.

Let us now consider temperatures close to the transition temperature

$$T_c{\rm Gi} \ll T - T_c \ll T_c. \quad (64)$$

Here, Gi $\sim t_c$ is the Ginzburg-Levanyuk number (see Ref. [40] for details). The first condition here stems from the range of the applicability of the one-loop RG for the coupling constants $|\gamma_c|t < 1$ [16] [see discussion below Eqs. (47)–(51)].

In addition to renormalization of the average LDOS given by Eq. (24), there are fluctuation corrections due to the Cooper-channel interaction of a non-RG type. Within the one-loop approximation, fluctuation corrections stem from the second line of Eq. (21) with frequency and moment integration restricted to the range $Dq^2,|\omega| \lesssim \max\{T_c,|E|\}$. In what follows, we shall term such contributions as those of real processes.

In order to take such fluctuation corrections accurately, one needs to renormalize the NLSM action down to the energy scale $\max\{T,|E|\}$ and, then, to evaluate the contribution in the second line of Eq. (21) with the renormalized parameters.[1]

This way, one finds

$$\frac{\langle\rho(E)\rangle}{\rho_0} = Z_s^{1/2}(T)[1-8(1-\ln 2)t_c(T_c\tau_{\rm GL})^2] \qquad (65)$$

for $|E| \ll \tau_{GL}^{-1}$,

$$\frac{\langle\rho(E)\rangle}{\rho_0} = Z_s^{1/2}(T)\left[1+2t_c\frac{T_c^2}{E^2}\ln(|E|\tau_{\rm GL})\right] \qquad (66)$$

for $\tau_{GL}^{-1} \ll |E| \ll T_c$, and

$$\frac{\langle\rho(E)\rangle}{\rho_0} = Z_s^{1/2}(|E|)\left[1+2t(L_E)\frac{T_c^2}{E^2}\ln(T_c\tau_{\rm GL})\right]$$
$$\simeq 1+2t(L_E)\frac{T_c^2}{E^2}\ln(T_c\tau_{\rm GL}) - \frac{3t^2(L_E)}{2t_c} \qquad (67)$$

for $T_c \ll |E| \ll 1/\tau$. Here, we have introduced the Ginzburg-Landau time as

$$\tau_{\rm GL}^{-1} = 8T_c|\gamma^{-1}(L_T)|/\pi. \qquad (68)$$

For the standard BCS-type divergence of γ_c, e.g., as in Eq. (57), $\tau_{\rm GL}^{-1} \sim T - T_c$, as usual. Expressions (65)–(67) were derived under assumption $T_c\tau_{\rm GL} \gg 1$.

To find the renormalization factor $Z_s(T)$ (with the subscript "s" emphasizing that the interaction is short ranged), we should integrate the RG equations (47)–(50) and (24). In the considered range of temperatures close to T_c [Eq. (64)], this, strictly speaking, cannot be done analytically, so that one should perform the integration numerically. In order to have an analytical approximation, we have used simplified RG equations (52), (57), and (61), which yield

$$Z_s^{1/2}(T) = e^{3t(L_T)-3t_0}\left[\frac{t_c - t(L_T)}{t_c - t_0}\right]^{3t_c}. \qquad (69)$$

Since we consider temperatures close to T_c, it is convenient to express $Z_s^{1/2}(T)$ via the Ginzburg-Landau time

$$Z_s^{1/2}(T) = \left(\frac{16}{3\pi e}\frac{T_c\tau_{\rm GL}}{t_c}\right)^{-3t_c}. \qquad (70)$$

We have checked that this analytical approximation is in reasonable agreement with the result of numerical integration of the exact RG equations. The renormalization factor $Z_s^{1/2}(|E|)$ is obtained from Eq. (69) by substitution L_E for L_T. The last term in the right-hand side of Eq. (67) is due to renormalization of $\langle\rho(E)\rangle$ from the energy scale $1/\tau$ down to $|E|$, in accordance with Eq. (62).

We mention that Eqs. (65)–(67) after the substitutions $Z_s^{1/2}(T) \to 1$, $t(L_E) \to t_0$, and $t_c \to t_0$ transform into the well-known results of a plain perturbation theory [41–43]. For temperatures close to T_c, renormalization effects due to interplay of disorder and interaction yield the following two important novel features in comparison with perturbative results:

(i) strong suppression of the disorder-averaged LDOS already at energies $|E| \sim T$ [see Eq. (70)];

(ii) the Ginzburg-Levanyuk number is determined by the renormalized resistance t_c rather than the bare one t_0, Gi $\sim t_c$ (see Ref. [40] for details).

The dependence of the disorder-averaged LDOS on energy is shown in Fig. 1(a). The particularly strong energy dependence of the disorder-averaged LDOS appears at temperatures close to T_c. It is worth emphasizing that the renormalization due to the interplay of disorder and interactions almost eliminates coherence peaks, reducing them to a weak feature near $E \simeq \tau_{\rm GL}^{-1}$. Up to these wiggles, $\langle\rho(E)\rangle$ is a monotonously increasing function of energy [compare the dotted and solid blue curves in Fig. 1(a)]. Further, the renormalization effects result in a pronounced reduction of the disorder-averaged LDOS in comparison with ρ_0 also at much higher temperatures, $T \gg T_c$ [see the dashed red curve in Fig. 1(a)].

The suppression of low-energy DOS due to renormalization factor (70) becomes stronger when the disorder (i.e., t_0) increases, and the system approaches the SIT (where $t_c \sim 1$). This effect is further strengthened on the insulating side of SIT. The analysis is fully analogous to that performed below for the case of a system close to the Anderson transition (see Sec. V C and the blue curve in Fig. 5). Physically, there is a close similarity between this effect and the development of the Coulomb zero-bias anomaly (ZBA) into soft Coulomb gap on the metal-insulator crossover (or transition) in normal systems [18]. The difference is that in the present case the source of the renormalization-induced effects, the ZBA on the superconducting side and the soft gap on the insulating side, is the attractive interaction.

We also note that the results (65)–(67) are obtained as the lowest order of the expansion in the renormalized resistance. It is sufficient to keep these lowest-order corrections only if we are not too close to the transition temperature $T_c\tau_{\rm GL} \ll 1/\sqrt{\rm Gi} \sim 1/\sqrt{t_c}$ [44,45], i.e., when the fluctuation correction to the disorder-averaged LDOS is small. Importantly, the above condition justifying the perturbative treatment of the superconducting fluctuation corrections to the density of states is stronger than the border $|\gamma_c|t \sim 1$ of validity of the one-loop RG equations for the coupling constants. The situation is somewhat similar to what we encounter in the case of Coulomb interaction, where the interaction corrections to the density of states (resulting from effective gauge fluctuations) are stronger than the corrections to the conductivity (see Sec. IV C).

Let us now analyze the fluctuations of the LDOS for short-ranged interactions. Since the function m_q (with $q \geq 2$) does not involve corrections from real processes, within one-loop approximation its behavior at finite temperature and energy is fully determined by RG result (63) with t taken at the length scale $\min\{L_T,L_E\}$. According to Eq. (63), mesoscopic

[1] In fact, the renormalization of the resistivity t continues below the energy scale $\max\{T,|E|\}$ and stops at the scale given by the dephasing rate $1/\tau_\phi$ which is generically smaller than $\max\{T,|E|\}$. In what follows, for simplicity, we will disregard the difference between these scales, which in 2D systems amounts to ignoring extra logarithmic factors of the order of $\ln(1/t)$ in corrections to t.

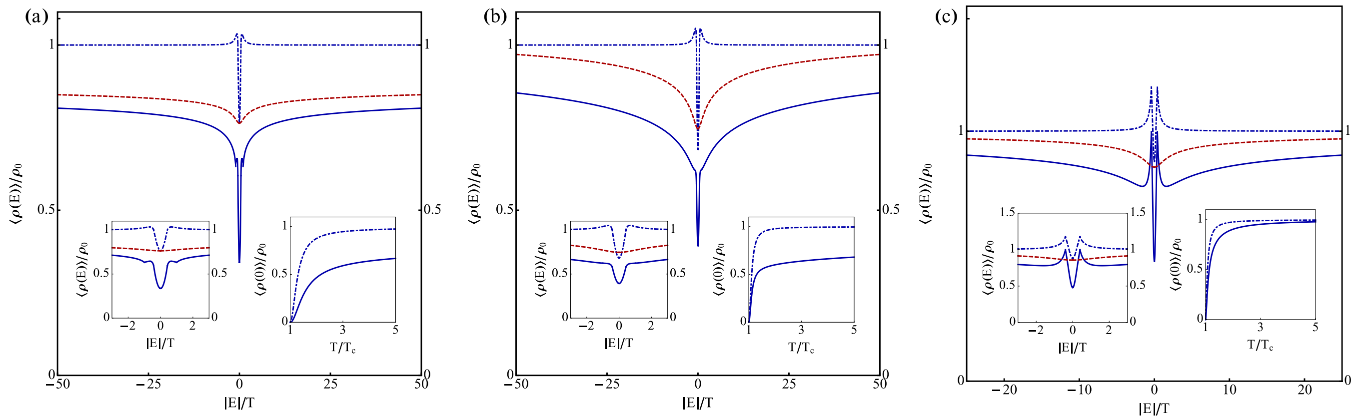

FIG. 1. Sketch of the disorder-averaged LDOS $\langle\rho(E)\rangle$ in the case of (a) short-range interaction, (b) Coulomb interaction, and (c) criticality. The solid blue curves correspond to the temperatures slightly above the superconducting transition temperature [$T = 1.6T_c$ for (a), $T = 1.2T_c$ for (b), and $T \gtrsim T_c^*$ for (c)]. The dotted-dashed blue curves are plotted for the same temperature as the solid blue curves according to the expressions which ignore renormalization between the ultraviolet energy scale $1/\tau$ and $\max\{T,|E|\}$. The dashed red curve is plotted for temperatures well above superconducting transition temperature [$T = 10T_c$ for (a) and (b), and $T \gg T_c^*$ for (c)]. The other parameters are (a) $t_c = 0.05$, $t_0 = 0.02$, and $T_c\tau_{\rm GL} = 2.5$; (b) $t_0 = 0.03$, $T_c\tau_{\rm GL} = 2.5$, and $\varkappa l = 0.2$. For all three figures, the left inset is enlarged view of dependence of $\langle\rho(E)\rangle$ on $|E|/T$ and the right inset is dependence of the disorder-averaged LDOS at $E = 0$ on temperature. See text and Eqs. (62), (65)–(67) for (a), Eqs. (76)–(78) for (b), and Eqs. (100) and (103) for (c) [46].

fluctuations of the LDOS are most pronounced at temperatures close to the superconducting transition temperature $T - T_c \ll T_c$. Using Eqs. (52) and (63), we obtain

$$\frac{\langle\rho^q(E)\rangle}{\langle\rho(E)\rangle^q} = \left(\frac{t_c}{t_0}\right)^{q(q-1)} \tag{71}$$

for $|E| \ll T_c$ and

$$\frac{\langle\rho^q(E)\rangle}{\langle\rho(E)\rangle^q} = \left(\frac{t_c}{t_0}\right)^{q(q-1)}\left(1+\frac{t_c}{2}\ln\frac{E}{T_c}\right)^{q(1-q)} \tag{72}$$

for $T_c \ll |E|$. This result implies that at energies $|E| < T_c$, fluctuations of the LDOS are large and non-Gaussian. For $|E| > T_c$, their amplitude decreases with increasing energy. The LDOS fluctuations are particularly strong for weak initial couplings satisfying $|\gamma_0| \ll t_0 \ll \sqrt{|\gamma_0|}$ (which is the range of parameters where the enhancement of T_c takes place) since in this case $t_c \gg t_0$. The fluctuations remain strong, for T close to T_c, also for intermediate initial couplings, as found from numerical solution of the full RG equations. To illustrate this, we show in Fig. 2 the ratio $\sqrt{\langle\rho^2(E)\rangle}/\langle\rho(E)\rangle$ obtained by numerical integration of Eqs. (47)–(50) and Eq. (45) for $q = 2$ [neglecting the two-loop contribution in Eq. (45)].

Finally, we note in passing that there is a fluctuation correction to m_q in the two-loop approximation. The two-loop correction to $[P_2^{\alpha_1\alpha_2}]^{RA}$ [see Eq. (A10)] can be cast as renormalization of the one-loop mesoscopic diffuson and cooperon (see Appendix B). Therefore, it does not produce fluctuation corrections to m_q. The two-loop renormalization of $[P_2^{\alpha_1\alpha_2}]^{RR}$ contains the contribution due to real processes in the Cooper channel [see Eq. (A3)]. However, as one can check, it leads to a correction which is by factor $t_c \ln T_c\tau_{\rm GL} \ll 1$ smaller than the fluctuation corrections to the disorder-averaged LDOS.

C. Coulomb interaction in 2D

Let us now consider the case of Coulomb interaction combined with weak attraction in the Cooper channel. For simplicity, we assume that the spin-rotational symmetry is fully broken such that the triplet channel is absent, $\mathcal{N} = 0$. Then, the full set of RG equations (47)–(50) can be reduced to

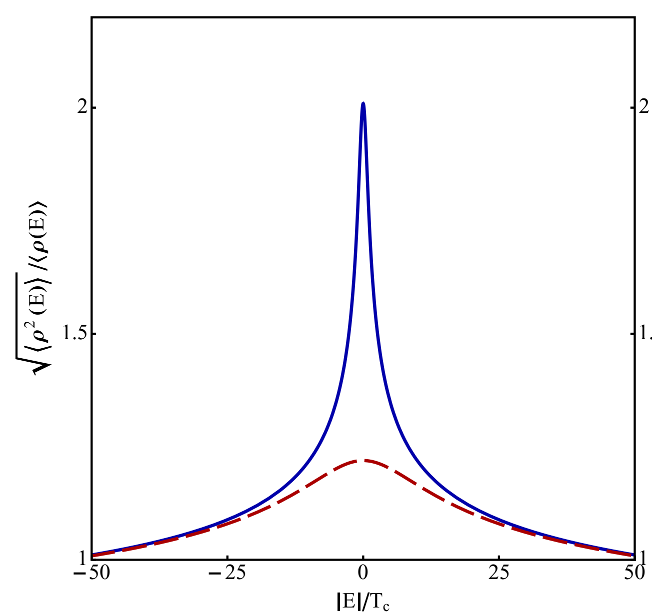

FIG. 2. Ratio $\sqrt{\langle\rho^2(E)\rangle}/\langle\rho(E)\rangle$ characterizing the magnitude of LDOS fluctuations in the case of short-range interaction. The curves are obtained by the numerical solution of RG equations (47)–(50) and (45) with initial values $t_0 = 0.2$ and $\gamma_{c0} = \gamma_{t0} = -\gamma_{s0} = -0.2$. The solid blue curve corresponds to the temperature $T \simeq T_c$. The dashed red curve is plotted for $T = 10T_c$.

the following system of two equations [47,48]:

$$\frac{dt}{dy} = \frac{t^2}{2}, \quad \frac{d\gamma_c}{dy} = \frac{t}{2} - 2\gamma_c^2. \tag{73}$$

Here, we neglect terms, which are powers of γ_c, as compared to unity. Equations (73) predict that in the weak coupling region $t_0, |\gamma_{c,0}| \ll 1$, superconductivity exists for $t_0 < 4\gamma_{c,0}^2$. The Cooper channel attraction becomes of the order of unity at the length scale [49]

$$y_c = \frac{1}{2\sqrt{t_0}} \ln \frac{2|\gamma_{c,0}| + \sqrt{t_0}}{2|\gamma_{c,0}| - \sqrt{t_0}} \gg 1. \tag{74}$$

We first consider the region of the phase diagram away from the separatrix $t_0 = 4\gamma_{c,0}^2$, when the following inequality holds: $y_c \ll 1/t_0$. The resistance $t_c = t(y_c)$ at this scale is not very different from t_0:

$$t_c = t_0\left(1 + \frac{\sqrt{t_0}}{4} \ln \frac{2|\gamma_{c,0}| + \sqrt{t_0}}{2|\gamma_{c,0}| - \sqrt{t_0}}\right) \sim t_0 \ll 1. \tag{75}$$

Therefore, one can expect that beyond the length scale y_c the superconducting instability develops under RG flow. The transition temperature to the superconducting phase can be estimated as $T_c \sim \tau^{-1} \exp(-2y_c)$. Due to the combined effect of disorder and Coulomb interaction, the transition temperature T_c decreases with growing t_0 from T_c^{BCS} at $t_0 = 0$ to 0 at $t_0 = 4\gamma_{c,0}^2$ [49].

In the considered case of Coulomb interaction, the disorder-averaged LDOS is dominated by the first term (which is formally infinite for $\gamma_s = -1$) in the right-hand side of Eq. (24). In fact, this means that the disorder-averaged LDOS is strongly suppressed by gauge-type fluctuations [22,34]. Taking into account corrections due to interaction in the Cooper channel [41–43] which become important only at temperatures close to the superconducting transition temperature $T - T_c \ll T_c$, we find

$$\frac{\langle\rho(E)\rangle}{\rho_0} = Z_c^{1/2}(T_c)[1 - 8(1 - \ln 2)t_c(T_c\tau_{\mathrm{GL}})^2] \tag{76}$$

for $|E| \ll \tau_{\mathrm{GL}}^{-1}$,

$$\frac{\langle\rho(E)\rangle}{\rho_0} = Z_c^{1/2}(T_c)\left[1 + 2\frac{t_c T_c^2}{E^2}\ln(|E|\tau_{\mathrm{GL}})\right] \tag{77}$$

for $\tau_{\mathrm{GL}}^{-1} \ll |E| \ll T_c$, and

$$\frac{\langle\rho(E)\rangle}{\rho_0} = Z_c^{1/2}(|E|)\left[1 + 2\frac{t(L_E)T_c^2}{E^2}\ln(T_c\tau_{\mathrm{GL}})\right] \tag{78}$$

for $T_c \ll |E|$. Here, the function $Z_c^{1/2}(|E|)$ describes the zero-bias anomaly for Coulomb interaction (hence the subscript c) and is given by [22,34,50,51]

$$Z_c^{1/2}(|E|) = \exp\left[-\frac{t_0}{4}\ln(E\tau)\ln\frac{E\tau}{\varkappa^2 l^2}\right], \tag{79}$$

where $\varkappa = (2\pi e^2/\varepsilon)dn/d\mu$ stands for the inverse static screening length in a 2D electron system. The renormalization factor $Z_c^{1/2}(T_c)$ is obtained by substitution of T_c for $|E|$ in Eq. (79). It can be estimated as

$$Z_c^{1/2}(T_c) = \exp\biggl[-\frac{1}{4}\ln\left(\frac{2|\gamma_{c,0}| - \sqrt{t_0}}{2|\gamma_{c,0}| + \sqrt{t_0}}\right) \times \ln\left(\frac{2|\gamma_{c,0}| - \sqrt{t_0}}{2|\gamma_{c,0}| + \sqrt{t_0}}(\varkappa l)^{-2\sqrt{t_0}}\right)\biggr] \ll 1. \tag{80}$$

At temperatures $T \gg T_c$ the disorder-averaged LDOS is fully determined by the zero-bias anomaly

$$\langle\rho(E)\rangle/\rho_0 = Z_c^{1/2}(\max\{|E|, T\}), \quad T \gg T_c. \tag{81}$$

We note that Eqs. (76)–(78) after the following substitutions, $Z_c^{1/2} \to 1$, $t(L_E) \to t_0$, and $t_c \to t_0$, transform into the well-known results of naive perturbation theory [41–43]. It is also worth mentioning that the renormalization of the disorder-averaged LDOS due to attraction in the Cooper channel [the term proportional to γ_c in Eq. (24)] is not important. As one can check, the Cooper channel term yields the contribution to $\ln Z_c^{1/2}(T_c)$ which is the factor $\sqrt{t_0}y_c \ll 1$ smaller than the zero bias anomaly contribution (80).

The dependence of the disorder-averaged LDOS on energy is shown in Fig. 1(b). The pronounced energy dependence of the disorder-averaged LDOS appears at temperatures close to T_c. The overall behavior of $\langle\rho(E)\rangle$ with energy is similar to the case of short-ranged interaction [see Fig. 1(b)]. At the same time, we emphasize the important difference between the two cases. For short-ranged interaction, the suppression of $\langle\rho(E)\rangle$ both at energies $|E| \gtrsim T_c$ and at $|E| \lesssim \tau_{\mathrm{GL}}^{-1}$ is controlled by the attractive interaction. Contrary to this, in the case of Coulomb interaction, the suppression of LDOS at energies $|E| \gtrsim T_c$ is dominated by the zero-bias anomaly factor $Z_c^{1/2}(E)$, whereas at $|E| \lesssim \tau_{\mathrm{GL}}^{-1}$ the suppression of $\langle\rho(E)\rangle$ is due to Cooper channel attraction. It is worth mentioning that, parametrically, the Coulomb renormalization factor (79) may lead to a much stronger suppression of LDOS than the attractive-interaction renormalization factor (70). On the other hand, for realistic parameters, this difference is usually not so dramatic [cf. Figs. 1(a) and 1(b)].

The two-loop result (45) for the anomalous dimension of the qth moment of LDOS for the case of Coulomb interaction takes the following form:

$$\frac{d\ln m_q}{dy} = \frac{q(q-1)}{8}\left[2t + \left(2 - \frac{\pi^2}{6} - 2\gamma_c\right)t^2\right]. \tag{82}$$

In the considered case, one can neglect the two-loop contribution. Using Eq. (73), we find the following one-loop RG result from Eq. (82):

$$m_q = (t/t_0)^{q(q-1)/2}. \tag{83}$$

Hence, for the disorder-averaged moments of LDOS at temperatures close to the superconducting temperature $T - T_c \ll T_c$,

$$\frac{\langle\rho^q(E)\rangle}{\langle\rho(E)\rangle^q} = \left(\frac{t_c}{t_0}\right)^{\frac{q(q-1)}{2}} \tag{84}$$

for $|E| \ll T$ and

$$\frac{\langle\rho^q(E)\rangle}{\langle\rho(E)\rangle^q} = \left(\frac{t_c}{t_0}\right)^{\frac{q(q-1)}{2}}\left(1 + \frac{t_c}{4}\ln\frac{E}{T}\right)^{\frac{q(1-q)}{2}} \tag{85}$$

for $T \ll |E|$.

When the initial couplings are weak, then, according to Eq. (75), t_c is typically close to t_0, exceeding it only slightly. Therefore, the mesoscopic fluctuations of LDOS in a problem with Coulomb interaction are in general weak for weak bare couplings. The only exception is a vicinity of the SIT separatrix $t_0 = 4\gamma_{c,0}^2$, such that

$$\ln \frac{2\sqrt{t_0}}{2|\gamma_{c,0}| - \sqrt{t_0}} \gtrsim 1/\sqrt{t_0}.$$

In this regime $t_c \gg t_0$, so that the LDOS fluctuations (85) become parametrically strong. This should be contrasted with the case of short-range interaction, for which there is a parametrically broad regime $|\gamma_0| \ll t_0 \ll \sqrt{|\gamma_0|}$ of very strong fluctuations (see Sec. IV B). For intermediate values of bare couplings, the LDOS fluctuations can be quantified, in full analogy with the short-range-interaction case, by a numerical solution of the RG equations. In Fig. 3, we display typical results obtained by numerical integration of Eqs. (47)–(50) (with $\mathcal{N} = 0$) and Eq. (46) (with $q = 2$ and neglecting the two-loop contribution). A comparison of Figs. 2 and 3 demonstrates that the LDOS fluctuations in the Coulomb case are weaker than in the short-range case with similar parameters. At $T \gg T_c$, the qth moment of LDOS is given by Eq. (83) with t taken at the length scale $\min\{L_T, L_E\}$.

Recently, mesoscopic fluctuations of the cooperon have been analyzed [52]. This study has revealed that the typical scale of fluctuations of the transition temperature to the superconducting state can be estimated as $\delta T_c/T_c \sim t_0^2\gamma_{c,0}^2/(4\gamma_{c,0}^2 - t_0)$. Near the separatrix, $4\gamma_{c,0}^2 - t_0 \ll t_0^3$, the fluctuations of the transition temperature become large, $\delta T_c/T_c \gg 1$. We mention that the mesoscopic fluctuations of the LDOS remain small at $t_0 \exp(-1/\sqrt{t_0}) \lesssim 4\gamma_{c,0}^2 - t_0 \ll t_0^3$.

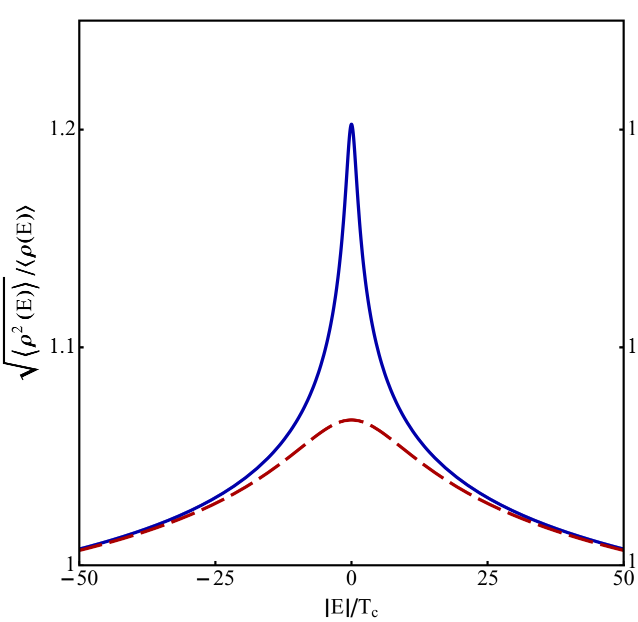

FIG. 3. Ratio $\sqrt{\langle\rho^2(E)\rangle}/\langle\rho(E)\rangle$ characterizing the magnitude of LDOS fluctuations in the case of Coulomb interaction. The curves are obtained by the numerical solution of RG equations (47)–(50) (with $\mathcal{N} = 0$) and Eq. (45) with initial values $t_0 = 0.25$ and $\gamma_{c0} = -0.35$. The solid blue curve corresponds to the temperature $T \simeq T_c$. The dashed red curve is plotted for $T = 10T_c$.

V. SYSTEM AT OR NEAR A NONINTERACTING ANDERSON TRANSITION

Let us now consider the case of weak short-range interactions, assuming that in the absence of interactions the system is near the Anderson transition. The physical examples include a 2D electron system with broken spin-rotational symmetry (class AII) or 3D electron systems with preserved or broken spin-rotational symmetry (classes AI and AII, respectively). For the sake of concreteness, we assume that the spin-rotational symmetry is not broken.

Since we assume that we start from weak interactions, the term describing the usual BCS instability is not important initially. Then, similar to Eqs. (53), during the first part of the RG evolution the coupling constants γ_s and γ_t adjust themselves to γ_c according to $\gamma_s = -\gamma_t = -\gamma_c \equiv -\gamma$ (the BCS line). Then, the superconducting instability can be described by single equation for γ:

$$\frac{d\gamma}{dy} = -\Delta_2\gamma - a\gamma^2. \tag{86}$$

Here, $\Delta_2 < 0$ stands for the multifractal exponent of the inverse participation ratio (bilinear in Q operator K_2) at the noninteracting fixed point describing the Anderson transition. For the case of 3D Anderson transition in class AI numerical simulations yield the estimate $\Delta_2 = -1.7 \pm 0.05$ [53]. The constant a is a universal number which is determined by the properties of composite operators at the noninteracting fixed point (cf. Ref. [54]). As follows from Eqs. (48)–(50), for $t \ll 1$ (i.e., at the critical point in $2+\epsilon$ dimensions), the coefficient a is positive, $a = 2/3 - t > 0$.

We note that Eq. (86) is written under the assumption that the attraction is weak, $|\gamma| \ll 1$. As one can see from Eq. (50), disorder generates higher powers of γ on the right-hand side of Eq. (86). In our analysis below, we assume that Eq. (86) describes the renormalization of γ both in the limit of weak and large attraction (see Ref. [40] for details). In other words, we assume that even in the presence of disorder, the superconducting instability occurs via the BCS scenario. This implies $a > 0$ in Eq. (86). We emphasize that, within this assumption, the analysis below is not sensitive to the details of the RG equation for intermediate values of γ.

Interactions affect the renormalization of the resistivity near the Anderson transition point. The corresponding RG equation for $\gamma \ll 1$ can be written as follows:

$$\frac{dt}{dy} = \frac{1}{\nu}(t - t_*) + \eta\gamma. \tag{87}$$

Here, $t_* \sim 1$ is the critical value of the resistivity in the noninteracting case. The second term with η generalizes the Altshuler-Aronov conductivity correction. In Eq. (87), we take in account that the presence of interactions drives the system away from the noninteracting critical point. In analogy with the coefficient a in Eq. (86), the constant η is a universal characteristics of the noninteracting fixed point. In general, η can be a positive or negative number of the order unity. The noninteracting correlation length exponent is positive,

$\nu > 0$. For the 3D Anderson transition in the presence of spin-rotational symmetry, numerical simulations yield the value $\nu = 1.57 \pm 0.02$ [55,56].

We now proceed in the same two-step manner, as before. For initially weak interaction, neglecting the term of the second order in γ, Eqs. (86) and (87) can be solved. For $|\Delta_2|\nu \neq 1$ we find

$$t = \tilde{t} + \frac{\eta\nu}{|\Delta_2|\nu - 1}\gamma, \quad (88)$$

where

$$\tilde{t} = t_* + (\tilde{t}_0 - t_*)e^{y/\nu}, \quad \gamma = \gamma_0 e^{|\Delta_2|y}, \quad (89)$$

and

$$\tilde{t}_0 = t_0 - \frac{\eta\nu\gamma_0}{|\Delta_2|\nu - 1}. \quad (90)$$

Therefore, in the presence of attractive interaction, the proper scaling variable is $\tilde{t}$ rather than t. However, since we assume that $|\gamma_0| \ll 1$ whereas $t_0 \sim t_* \sim 1$ the difference between t_* and $\tilde{t}_c = t_* - \eta\nu\gamma_0/(|\Delta_2|\nu - 1)$ is small.

In the special case $|\Delta_2|\nu = 1$, we find

$$\tilde{t} = t - \eta\gamma_0\gamma y, \quad \tilde{t}_0 = t_0. \quad (91)$$

In what follows, we shall omit "tilde" sign and neglect the difference between $\tilde{t}_*$ and t_*.

At finite temperature, the RG flow given by Eq. (86) terminates at the length scale $L_T = l(T\tau)^{-1/d}$. Solving Eq. (86), we find the following estimate for the temperature of transition to the superconducting state:

$$T_c^* = \tau^{-1}e^{-dy_c} = \frac{1}{\tau}\left(\frac{a|\gamma_0|}{|\Delta_2|}\right)^{d/|\Delta_2|}. \quad (92)$$

For $t < t_*$ the resistance decreases under RG flow. At the scale $\xi = l|t_0/t_* - 1|^{-\nu}$ the resistance vanishes, whereas the Cooper-channel interaction becomes

$$\gamma(\xi) = \gamma_0(\xi/l)^{|\Delta_2|}. \quad (93)$$

After this (in view of $t = 0$), the further renormalization of γ is controlled by the standard disorder-free BCS mechanism. Then, the transition temperature can be estimated as

$$T_c(\xi) = \delta_\xi e^{-1/|\gamma(\xi)|} = \delta_\xi \exp\left[-\frac{a}{|\Delta_2|}\left(\frac{T_c^*}{\delta_\xi}\right)^{\Delta_2/d}\right], \quad (94)$$

where $\delta_\xi = \tau^{-1}(\xi/l)^{-d}$ stands for the typical level spacing in the volume of linear size ξ. This expression for $T_c(\xi)$ interpolates between $T_c(\xi) \sim T_c^*$ at $\delta_\xi \sim T_c^*$ and $T_c(\xi) \sim T_c^{\mathrm{BCS}}$ at $\delta_\xi \sim 1/\tau$.

For $t > t_*$, in the absence of attraction the system would be in the insulating phase. In the presence of interaction in the Cooper channel, the RG flow proceeds in accordance with Eqs. (86) and (87) up to the localization length ξ. There are two possibilities. If $L_* = l\exp(y_c) < \xi$, the attraction becomes of the order of unity in the critical region of noninteracting Anderson transition. Then, one expects that the superconducting phase establishes below temperature T_c^*. In the opposite case $L_* > \xi$, the localization takes place first, and superconductivity is not developed. Thus, the relation

$$\delta_\xi \sim T_c^* \Leftrightarrow |\gamma_0| \sim (t_* - t_0)^{\nu|\Delta_2|} \quad (95)$$

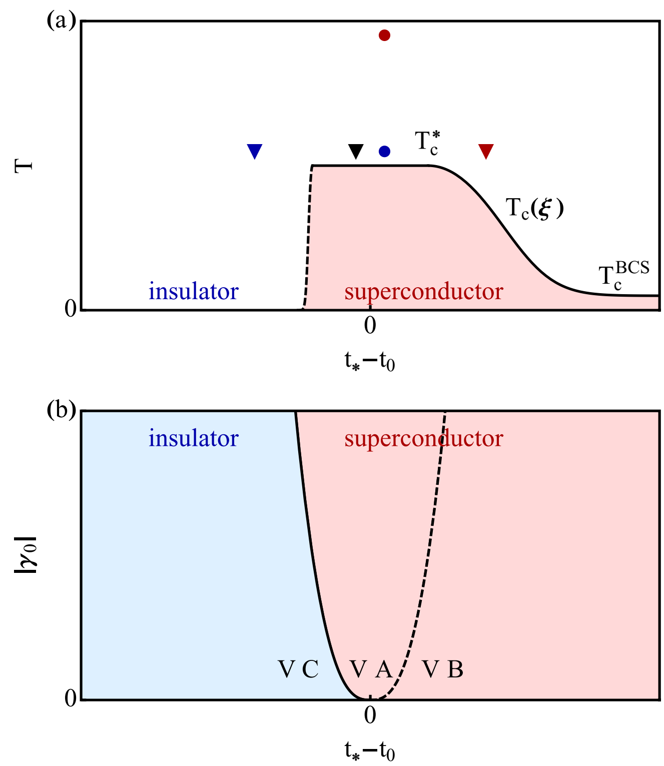

FIG. 4. (a) Sketch of the superconducting transition temperature as a function of distance from the critical point $t_0 - t_*$ at fixed value of bare attraction γ_0 [see Eqs. (92) and (94)]. The red and blue dots correspond to the temperatures at which the energy dependencies of LDOS in Fig. 1(c) are shown. The blue, black, and red triangles correspond to curves $\langle\rho(E)\rangle$ shown in Fig. 5. (b) Schematic phase diagram in the interaction-disorder plane near the critical point. Solid black curve denotes the superconductor-insulator transition. The symbols "V A," "V B," and "V C" mark regions of the phase diagram in which behavior of LDOS is discussed in corresponding sections.

is the condition of the superconductor-insulator transition (at zero temperature) (see Fig. 4). It is worth noting that Ref. [14] argues that superconducting state with $T_c \ll T_c^*$ persists further in the localized regime ($\delta_\xi > T_c^*$) due to Mott-type rare configurations. Our RG approach (at least, in its present form) is not sufficient to explore this possibility.

A. Exactly at criticality

On the BCS line (56), the renormalization of the local density of states near the Anderson transition fixed point can be described by the following equation:

$$\frac{d\ln\rho}{dy} = b\gamma, \quad (96)$$

where the coefficient b is determined by the scaling properties of the Finkel'stein term at the noninteracting fixed point. As follows from Eq. (61), at $t \ll 1$, the coefficient b is positive, $b = 2t > 0$. Below we assume that it is positive in general. We emphasize that there is no renormalization of the local density of states in the absence of interaction. The flow described by the RG equation (96) is stopped at the length scale $\mathcal{L} = \min\{L_T, L_E\}$ where $L_E = l(|E|\tau)^{-1/d}$.

We start our analysis of the disorder-averaged LDOS at the criticality $\delta_\xi \ll T_c^*$. At temperatures higher than the superconducting transition temperature $T \gg T_c^*$, we can solve Eqs. (86) and (96) for $|\gamma| \ll 1$:

$$\frac{\langle\rho(E)\rangle}{\rho_0} = 1 + \frac{b}{|\Delta_2|}(\gamma - \gamma_0). \tag{97}$$

Hence, we find the following behavior of the disorder-averaged LDOS in the critical region:

$$\frac{\langle\rho(E)\rangle}{\rho_0} = 1 - \frac{b}{a}\left(\frac{T_c^*}{|E|}\right)^{|\Delta_2|/d} + \frac{b}{a}(T_c^*\tau)^{|\Delta_2|/d} \tag{98}$$

for $|E| \gg T \gg T_c^*$ and

$$\frac{\langle\rho(E)\rangle}{\rho_0} = 1 - \frac{b}{a}\left(\frac{T_c^*}{T}\right)^{|\Delta_2|/d} + \frac{b}{a}(T_c^*\tau)^{|\Delta_2|/d} \tag{99}$$

for $T \gg |E| \gg T_c^*$. Thus, there is a relatively small depletion of the disorder-averaged LDOS at temperatures $T \gg T_c^*$ [see red line in Fig. 1(c)].

When temperature is close to the superconducting transition temperature $T - T_c^* \ll T_c^*$, the energy dependence of the disorder-averaged LDOS is described by expressions analogous to Eqs. (65)–(67):

$$\frac{\langle\rho(E)\rangle}{\rho_0} = Z_*^{1/2}(T) \times \begin{cases} 1 - c_d t_* [T_c^*\tau_{\rm GL}]^{\frac{6-d}{2}}, & |E| \ll \tau_{\rm GL}^{-1}, \\ 1 + \tilde{c}_d t_* \left[\frac{T_c^*}{|E|}\right]^{\frac{6-d}{2}}, & \tau_{\rm GL}^{-1} \ll |E| \ll T_c^*. \end{cases} \tag{100}$$

The numerical coefficients c_d and $\tilde{c}_d$ are of the order unity and are given in Appendix C. The function

$$Z_*^{1/2}(T) = \left[\frac{\Delta_2 + a\gamma_0}{\Delta_2 + a\gamma(L_T)}\right]^{b/a} \tag{101}$$

can be estimated for temperatures close to T_c^* as

$$Z_*^{1/2}(T) = \left(\frac{8a}{\pi|\Delta_2|}T_c^*\tau_{\rm GL}\right)^{-b/a}. \tag{102}$$

At energies $\tau^{-1} \gg |E| \gg T_c^*$, the disorder-averaged LDOS is given by

$$\frac{\langle\rho(E)\rangle}{\rho_0} = 1 - \frac{b}{a}\left(\frac{T_c^*}{|E|}\right)^{\frac{|\Delta_2|}{d}} + \tilde{c}_d t_*\left(\frac{T_c^*}{|E|}\right)^{\frac{6-d}{2}}. \tag{103}$$

The fluctuation correction [the last term on the right-hand side of Eq. (103)] is small in comparison with the RG correction [the second term on the right-hand side of Eq. (103)] provided the following inequality holds: $2|\Delta_2| < d(6-d)$. The latter is true for $d = 3$. The LDOS at a temperature T close to T_c is shown by the full blue line in Fig. 1(c). The curves show a strong suppression of LDOS near zero energy as well as clear precursors of coherence peaks at $|E| \sim \tau_{\rm GL}^{-1}$.

We note that, strictly speaking, our results (100) are valid under the condition that the critical resistance is small $t_* \ll 1$. Only in this case, there is a wide range of applicability for Eq. (100), $1 \ll T_c^*\tau_{\rm GL} \ll t_*^{-2/(6-d)}$. For $t_* \sim 1$, the results indicate that already at $T_c^*\tau_{\rm GL} \sim 1$ there is strong suppression of the disorder-averaged LDOS. In this case, one needs to sum up higher-order contributions coming from the superconducting fluctuations.

The scaling behavior of the qth moment of LDOS can be described by the following RG equation:

$$\frac{d\ln m_q}{dy} = -\Delta_q + b_q\gamma. \tag{104}$$

The perturbative result (45) implies $b_q = q(1-q)t^2 < 0$ for $q > 1$. We remind the reader that at finite energy and temperature, the RG flow [Eq. (104)] stops at the length scale $\mathcal{L}$. At larger scales, the interaction correction disappears from Eq. (104) and the scaling of m_q is exactly the same as without interaction up to the length scale $L_\phi \sim \tau_\phi^{1/d}$ induced by the interaction (see Appendix B). We expect a power-law dependence of τ_ϕ on energy and temperature $\tau_\phi \sim (\max\{|E|,T\})^{-p}$.

The solution of Eqs. (86) and (104) provides, in particular, the following result for the temperature/energy dependence of m_q:

$$m_q = \left(\frac{\mathcal{L}}{L_\phi}\right)^{\Delta_q}\left(\frac{\gamma(\mathcal{L})}{\gamma_0}\right)^{\frac{\Delta_q}{\Delta_2}}\left(\frac{\Delta_2 + a\gamma_0}{\Delta_2 + a\gamma(\mathcal{L})}\right)^{x_q}, \tag{105}$$

where we introduce the exponent $x_q = b_q/a + \Delta_q/\Delta_2$. Here, we have taken into account that typically $L_\phi \gg \mathcal{L}$. Hence, at $T \gg T_c^*$ we obtain the following results for the moments of LDOS:

$$\frac{\langle\rho^q(E)\rangle}{\langle\rho(E)\rangle^q} = \left(\frac{\tau}{\tau_\phi}\right)^{\frac{\Delta_q}{d}}\left[1 - x_q\left(\frac{T_c^*}{|E|}\right)^{\frac{|\Delta_2|}{d}} + x_q(T_c^*\tau)^{\frac{|\Delta_2|}{d}}\right] \tag{106}$$

for $|E| \gg T \gg T_c^*$ and

$$\frac{\langle\rho^q(E)\rangle}{\langle\rho(E)\rangle^q} = \left(\frac{\tau}{\tau_\phi}\right)^{\frac{\Delta_q}{d}}\left[1 - x_q\left(\frac{T_c^*}{T}\right)^{\frac{|\Delta_2|}{d}} + x_q(T_c^*\tau)^{\frac{|\Delta_2|}{d}}\right] \tag{107}$$

for $T \gg |E| \gg T_c^*$. At temperatures close to the superconducting transition temperature $T - T_c^* \ll T_c^*$, the qth moment of the LDOS at energies $|E| \gg T \approx T_c^*$ is given by Eq. (106). At energies $|E| \ll T \approx T_c^*$, the qth moment of the LDOS can be estimated as

$$\frac{\langle\rho^q(E)\rangle}{\langle\rho(E)\rangle^q} = \left(\frac{\tau}{\tau_\phi^*}\right)^{\frac{\Delta_q}{d}}\left(\frac{8a}{\pi|\Delta_2|}T_c^*\tau_{\rm GL}\right)^{-\frac{b_q}{a}}. \tag{108}$$

Here, τ_ϕ^* is the dephasing time at $|E| \sim T \sim T_c^*$. We note that the moments of the normalized LDOS $\rho(E)/\langle\rho(E)\rangle$ are strongly enhanced at $|E| \sim T \sim T_c^*$ for $b_q < 0$. Provided a stronger condition is fulfilled, $b_q + qb < 0$, the moments $\langle\rho^q\rangle(E)$ are large at $|E| \sim T \sim T_c^*$ not only in comparison with $\langle\rho(E)\rangle^q$, but even in comparison with the bare value ρ_0^q.

B. Off criticality: Metallic/superconducting side

Let us now consider the metallic side of the Anderson transition $t_0 < t_*$. In this case, the system is a superconductor for temperatures below $T_c(\xi)$ given by Eq. (94). We will assume that the system is off criticality, in the sense that $\delta_\xi \gg T_c^*$, in which case $T_c(\xi) \ll T_c^*$. At high temperatures $T \gg T_c(\xi)$, the disorder-averaged LDOS reads as

$$\frac{\langle\rho(E)\rangle}{\rho_0} = 1 + \frac{b}{|\Delta_2|}\gamma(\xi)\left(\frac{\delta_\xi}{\max\{|E|,T,\delta_\xi\}}\right)^{\frac{|\Delta_2|}{d}}. \quad (109)$$

This result is the solution of RG equation (96) taken at the length scale $\min\{\xi,\mathcal{L}\}$. We note that the attraction interaction at the scale ξ can be expressed via the superconducting transition temperature: $\gamma(\xi) = 1/\ln[T_c(\xi)/\delta_\xi]$.

For temperatures close to $T_c(\xi)$, $T - T_c(\xi) \ll T_c(\xi)$, the disorder-averaged LDOS becomes

$$\frac{\langle\rho(E)\rangle}{\rho_0} = 1 + \frac{b}{|\Delta_2|}\gamma(\xi)\left(\frac{\delta_\xi}{|E|}\right)^{\frac{|\Delta_2|}{d}} + \tilde{c}_d t_*\left(\frac{T_c(\xi)}{|E|}\right)^{\frac{6-d}{2}} \quad (110)$$

for $|E| \gg \delta_\xi$ and

$$\frac{\langle\rho(E)\rangle}{\rho_0} = 1 + \frac{b}{|\Delta_2|}\gamma(\xi) \quad (111)$$

for $|E| \ll \delta_\xi$. We note that the energy dependence of the disorder-averaged LDOS for $|E| \gg \delta_\xi$ is the same as at the criticality [cf. Eqs. (98), (110), and (103)]. There is no disorder-induced fluctuation corrections like in Eq. (100) at energies $|E| \ll \delta_\xi$ since $t(\xi) = 0$.

The dependence of the qth moment of LDOS on energy and temperature at $T > T_c(\xi)$ is determined by the solution of RG equation (104):

$$\frac{\langle\rho^q(E)\rangle}{\langle\rho(E)\rangle^q} = \left(\frac{\gamma(\xi)}{\gamma_0}\right)^{\frac{\Delta_q}{\Delta_2}}(\min\{1,\delta_\xi\tau_\phi\})^{\frac{|\Delta_q|}{d}} \times\left[1 - \frac{x_q a}{\Delta_2}\gamma(\xi)\left(\min\left\{1,\frac{\delta_\xi}{|E|},\frac{\delta_\xi}{T}\right\}\right)^{\frac{|\Delta_2|}{d}}\right]. \quad (112)$$

We note that the dephasing rate here is affected by the superconducting fluctuations (see Appendix B).

C. Off criticality: Insulating side

Finally, let us consider the insulating phase of the Anderson transition $t_0 > t_*$. We will assume that we are sufficiently far from criticality, $\delta_\xi \gtrsim T_c^*$, in which case the system remains an insulator in the presence of attracting interaction (i.e., we are on the insulating side of SIT). For the sake of simplicity, we consider the zero-temperature regime $T = 0$. At high energies $\tau^{-1} \gg |E| \gg \delta_\xi$, the disorder-averaged LDOS can be found from Eqs. (86) and (96):

$$\frac{\langle\rho(E)\rangle}{\rho_0} = 1 + \frac{b}{|\Delta_2|}\gamma(\xi)\left(\frac{\delta_\xi}{|E|}\right)^{\frac{|\Delta_2|}{d}}. \quad (113)$$

We emphasize that $|\gamma(\xi)| \ll 1$ at $\delta_\xi \gg T_c^*$. We note that the result (113) is the same as Eq. (98) in which we neglect the last term on the right-hand side in comparison with the second one. Therefore, at high energies $|E| \gg \delta_\xi$, the energy dependence of the disorder-averaged LDOS is the same as in the critical region, $\delta_\xi \ll T_c^*$.

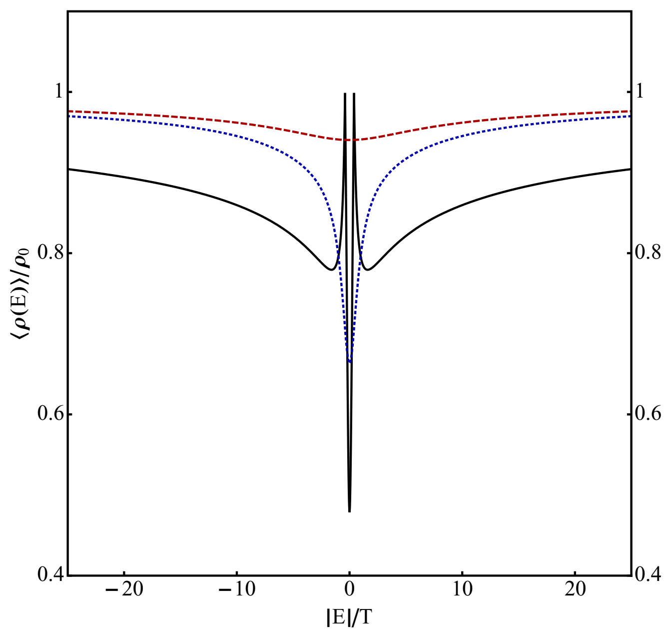

FIG. 5. Disorder-average LDOS $\langle\rho(E)\rangle$ across the SIT. All three curves correspond to the same temperature T, which is assumed to be slightly exceeding the superconducting transition temperature T_c^* at the Anderson transition [see triangles of the corresponding colors in Fig. 4(a)]. The dashed red curve corresponds to the metallic side of the Anderson transition $t_0 < t_*$, where the interacting system is a superconductor at low temperatures [Sec. V B, Eqs. (110) and (111)]. The solid black curve is the LDOS at criticality $t_0 = t_*$ [Sec. V A, Eqs. (100) and (103)], and the dotted blue curve is plotted for the insulating phase $t_0 > t_*$ [Sec. V C, Eq. (114)].

At $|E| \ll \delta_\xi$, one can still use Eq. (21), but taking into account the insulator-type behavior of the conductivity (cf. Ref. [18]). Then, we obtain (see Appendix C)

$$\frac{\langle\rho(E)\rangle}{\rho_0} = 1 - a_1|\gamma(\xi)|\left(\ln\frac{\delta_\xi}{|E|}\right)^{d+2} - a_2\gamma^2(\xi)\frac{\delta_\xi}{|E|}. \quad (114)$$

Here, a_1 and a_2 are positive constants. The last term on the right-hand side of Eq. (114) is small at $|E| \sim \delta_\xi$. With further lowering energy, it becomes larger than the second term in the energy interval $|\gamma(\xi)|\Delta_P \ll |E| \ll \Delta_P$, where

$$\Delta_P \sim |\gamma(\xi)|\delta_\xi \propto \xi^{-d-\Delta_2}. \quad (115)$$

We emphasize that the energy scale Δ_P coincides with the so-called pseudogap energy scale introduced in Ref. [14].

The behavior of the disorder-averaged LDOS $\langle\rho(E)\rangle$ across the SIT is shown in Fig. 5. All three curves in this figure correspond to the same temperature T, which is assumed to be slightly exceeding the superconducting transition temperature T_c^* at the Anderson transition [see triangles of the corresponding colors in Fig. 4(a)]. The red curve shows a weak depletion on the metallic side of the Anderson transition $t_0 < t_*$ (Sec. V B). Note that for this curve, the temperature T is much larger than the relevant superconducting temperature $T_c(\xi)$; the depletion becomes more pronounced when one reduces the temperature, approaching $T_c(\xi)$. The black curve corresponds to criticality, $t_0 = t_*$ (Sec. V A). It shows a much stronger suppression of LDOS around zero energy, accompanied by clear precursors of coherence peaks [as was already shown by solid blue curve in Fig. 1(c)]. Finally, the blue curve in Fig. 5 illustrates a strong "pseudogap" arising on the insulating side of the transition.

For high energies $\tau^{-1} \gg |E| \gg \delta_\xi$, the fluctuations of LDOS are controlled by the noninteracting fixed point at $t = t_*$. As in the critical region, the moments of LDOS are determined by the corresponding multifractal exponents Δ_q:

$$\frac{\langle \rho^q(E)\rangle}{\langle \rho(E)\rangle^q} = \left(\frac{\gamma(\xi)}{\gamma_0}\right)^{\frac{\Delta_q}{\Delta_2}} \left(\frac{\delta_\xi}{|E|}\right)^{\frac{|\Delta_q|}{d}} \times \left[1 - \frac{x_q a}{\Delta_2}\gamma(\xi)\left(\frac{\delta_\xi}{|E|}\right)^{\frac{|\Delta_2|}{d}}\right]. \tag{116}$$

We note that the last term in the square brackets on the right-hand side of Eq. (104) is much smaller than unity since the attractive interaction at the scale of localization length is weak, $|\gamma(\xi)| \ll 1$. When energy is below the level spacing in the localization volume $|E| \ll \delta_\xi$, the LDOS shows the multifractal behavior up to the scale ξ and, then, insulatorlike fluctuations up to the system size L:

$$\frac{\langle \rho^q(E)\rangle}{\langle \rho(E)\rangle^q} = \left(\frac{\gamma(\xi)}{\gamma_0}\right)^{\frac{\Delta_q}{\Delta_2}} \left(\frac{L}{\xi}\right)^{d(q-1)}. \tag{117}$$

At finite temperatures $T \ll |E|$, the insulatorlike fluctuations are regularized by the temperature-induced dephasing length $L_{\phi T}$.

VI. SUMMARY AND CONCLUSIONS

In conclusion, we have developed the theory of local density of states and its mesoscopic fluctuations near the transition to the superconducting state. Specifically, we considered systems on the superconducting side of SIT but at temperatures above T_c, as well as systems on the insulating side of SIT. We have employed the nonlinear sigma-model formalism and constructed the operators that describe the moments of the local density of states. Our strategy has combined the following two steps: (i) renormalization of these operators as well as the coupling constants of the action followed by (ii) including the superconducting fluctuations arising from real processes. In view of the length of the paper, we find it appropriate to list here the main results obtained in Secs. III–V, with the references to corresponding equations.

(1) In Sec. III, we have performed the two-loop renormalization of the moments of LDOS in the presence of interactions in the singlet and triplet particle-hole channels, as well as in the Cooper channel. The zeta function governing the renormalization of the qth moment of the LDOS is given by Eq. (45).

(2) In Sec. IV, we have used these two-loop results to study the scaling behavior of the disorder-averaged LDOS and its moments in 2D disordered films near the finite-temperature superconducting transition. For short-ranged interactions, the evolution of the average LDOS $\langle \rho(E)\rangle$ with increasing energy E is given by Eqs. (65)–(67) and illustrated in Fig. 1(a). We have found that the combined effect of renormalization and superconducting fluctuations progressively depletes the LDOS with lowering energy $|E|$ and suppresses the "coherence peaks."

(3) The scaling of the moments of the LDOS for short-range interactions is given by Eqs. (71) and (72). The LDOS fluctuations are particularly strong for weak initial couplings satisfying $|\gamma_0| \ll t_0 \ll \sqrt{|\gamma_0|}$, which is the range of parameters where the enhancement of T_c by multifractality takes place. A representative curve characterizing LDOS fluctuations for intermediate initial couplings shown in Fig. 2 demonstrates that the fluctuations are rather strong also in this regime.

(4) Further, in Sec. IV C, we have analyzed the LDOS in 2D superconducting films with long-range Coulomb repulsion. The superconducting transition temperature is then suppressed as compared to the clean case. The evolution of the average LDOS with energy is described by Eqs. (76)–(78) [see Fig. 1(b)], and is governed by the interplay of the Coulomb-induced zero-bias anomaly and superconducting fluctuations. The overall behavior of the LDOS is similar to the case of the short-range interactions [cf. Figs. 1(a) and 1(b)]. Mesoscopic fluctuations of the LDOS [Eqs. (84) and (85)] are found to be suppressed by the Coulomb repulsion. A representative curve characterizing LDOS fluctuations for intermediate initial couplings is shown in Fig. 3. The fluctuations are substantially weaker than for the case of short-range interaction with comparable bare couplings (Fig. 2) but remain quite sizable.

(5) In Sec. V, we have studied the LDOS near the superconducting transition in a system with weak short-ranged interactions which, in the absence of interactions, would be close to the Anderson metal-insulator transition. On the superconducting side, the average LDOS is described by Eqs. (109)–(111), and the scaling of its qth moment is given by Eq. (112). The average LDOS decreases with lowering of energy at high energies $|E| \gg \delta_\xi$, and saturates at $|E| \ll \delta_\xi$ (see Fig. 5). We neglected suppression of $\langle \rho(E)\rangle$ arising from the ballistic scales. At criticality, the average LDOS is given by Eqs. (100) and (103) and is strongly depleted around zero energy by superconducting fluctuations, as illustrated in Figs. 1(c) and 5. The corresponding LDOS fluctuations are described by Eqs. (106)–(108) and are strong for energies and temperatures of the order of critical temperature T_c^*.

(6) On the insulating side, the average LDOS is also strongly depleted [see Eqs. (113) and (114) and Fig. 5]. The energy scale Δ_P [Eq. (115)] which emerges as the characteristic scale in these formulas for $\langle \rho(E)\rangle$, resembles the pseudogap scale introduced in Ref. [14]. The LDOS fluctuations on the insulating side at high and low energies (compared to the level spacing in the localization volume) are given by Eqs. (116) and (117), respectively.

Let us now summarize on a qualitative level the most salient of these findings.

(1) We have observed a strong depletion of LDOS in two regimes: (i) on the superconducting side of SIT, above T_c, and (ii) on the insulating side of SIT.

(2) This depletion arises from a combination of two mechanisms: (i) renormalization effects that are operative at higher energies $E \gtrsim T$, and (ii) real processes due to superconducting fluctuations that are operative at lower energies $E \lesssim T$. The renormalization effects are governed by attractive interaction for systems with short-range interaction or by Coulomb interaction when it is present. Remarkably, the

resulting depletion of LDOS is qualitatively similar in these two cases.

(3) The interplay of renormalization effects and of superconducting fluctuations tends to suppress the precursors of coherence peaks.

(4) A substantial depletion of LDOS remains observable for temperatures much exceeding (by factor ~ 10) the superconducting transition temperature T_c.

(5) In a model with short-range interaction, multifractality leads to strong mesoscopic fluctuations of LDOS, which should be observable as point-to-point fluctuations when the surface of a system is scanned in an STM experiment. The Coulomb interaction reduces the magnitude of the mesoscopic fluctuations. However, also in a model with Coulomb interaction, the fluctuations become strong when the systems approach the SIT.

Our findings compare well with experimental observations of depletion of LDOS and of its large point-to-point fluctuations in the metallic and insulating phases near SIT in TiN, InO, and NbN films [3–8,57]. Let us emphasize that our results have been obtained entirely within the sigma-model formalism (usually referred to as a "fermionic approach") for a macroscopically homogeneous system. All the observed effects are thus intrinsic properties of this problem and do not require any additional assumptions, such as the presence of macroscopic inhomogeneities ("granularity").

ACKNOWLEDGMENTS

We thank M. V. Feigel'man, M. A. Skvortsov, and K. S. Tikhonov for useful discussions. The work was supported by the DFG and by the Russian Science Foundation under the Grant No. 14-42-00044.

APPENDIX A: TWO-LOOP CONTRIBUTION TO THE LDOS CORRELATION FUNCTION K_2

In this appendix, we present technical details of the calculation of the irreducible two-point LDOS correlation function K_2. We start with the evaluation of the two-loop contribution from $P_2^{\alpha_1\alpha_2}(i\varepsilon_{n_1},i\varepsilon_{n_3})$. In the two-loop approximation, one needs to take into account only the terms with four W:

$$\big[P_2^{\alpha_1\alpha_2}\big]^{(2)}\big(i\varepsilon_{n_1},i\varepsilon_{n_3}\big)=\frac{1}{4}\sum_{n_6n_8}\sum_{\beta_1\beta_2}\big[\big\langle\!\big\langle \mathrm{sp}\big[w^{\alpha_1\beta_1}_{n_1n_6}\bar{w}^{\beta_1\alpha_1}_{n_6n_1}\big]\mathrm{sp}\big[w^{\alpha_2\beta_2}_{n_3n_8}\bar{w}^{\beta_2\alpha_2}_{n_8n_3}\big]\big\rangle\!\big\rangle-2\,\mathrm{sp}\big\langle w^{\alpha_1\beta_1}_{n_1n6}\bar{w}^{\beta_1\alpha_2}_{n_6n_3}w^{\alpha_2\beta_2}_{n_3n_8}\bar{w}^{\beta_2\alpha_1}_{n_8n_1}\big\rangle\big]. \tag{A1}$$

By using Wick's theorem and Eqs. (12)–(15), we find

$$\begin{aligned}\big[P_2^{\alpha_1\alpha_2}\big]^{(2)}\big(i\varepsilon_{n_1},i\varepsilon_{n_3}\big)=&\frac{2^{12}\pi T}{g^3}\sum_{j=0}^{3}\Gamma_j\int_{q,p}\sum_{\omega_n>\varepsilon_{n_3}}\mathcal{D}_p(i\omega_n)\mathcal{D}_p^{(j)}(i\omega_n)\big[\mathcal{D}_q\big(i\omega_n+i\Omega^{\varepsilon}_{13}\big)+\mathcal{C}_q\big(i\omega_n+i\Omega^{\varepsilon}_{13}\big)\big]\\&+\frac{2^{13}\pi TZ_\omega}{g^3}\int_{q,p}\sum_{\omega_n<\varepsilon_{n_3}}\mathcal{C}_p^2\big(2i\varepsilon_{n_3}-i\omega_n\big)\mathcal{L}_p(i\omega_n)[\mathcal{D}_q(i\mathcal{E}_{13}-i\omega_n)+\mathcal{C}_q(i\mathcal{E}_{13}-i\omega_n)]+\big(\varepsilon_{n_1}\leftrightarrow\varepsilon_{n_3}\big).\end{aligned} \tag{A2}$$

Performing the analytical continuation to real frequencies $i\varepsilon_{n_1}\to E+i0^+$, $i\varepsilon_{n_3}\to E'+i0^+$, we obtain

$$\begin{aligned}\big[P_2^{\alpha_1\alpha_2}\big]^{RR(2)}(E,E')=&\frac{2^{11}}{ig^3}\sum_{j=0}^{3}\Gamma_j\int_{q,p,\omega}\mathcal{F}_{\omega-E'}\mathcal{D}^R_p(\omega)\mathcal{D}^{(j)R}_p(\omega)\mathcal{D}^R_q(\omega+\Omega)\\&+\frac{2^{12}Z_\omega}{ig^3}\int_{q,p,\omega}\mathcal{C}^{R2}_p(2E-\omega)\mathcal{C}^R_q(\mathcal{E}-\omega)\big[\mathcal{L}^K_p(\omega)+\mathcal{F}_{E-\omega}\mathcal{L}^R_p(\omega)\big]+(E\leftrightarrow E'),\end{aligned} \tag{A3}$$

where $\mathcal{E}=E+E'$. Here, we have taken into account that diffuson $\mathcal{D}^R_q(\omega)$ and cooperon $\mathcal{C}^R_q(\omega)$ propagators are the same. Setting $E=E'=T=0$, we find in $d=2+\epsilon$ dimensions (see details for evaluation of the integrals in Ref. [19])

$$\big[P_2^{\alpha_1\alpha_2}\big]^{RR(2)}\to 16\frac{t^2h^{2\epsilon}}{\epsilon^2}\left[2\gamma_c+\sum_{j=0}^{3}\ln(1+\gamma_j)-\frac{\epsilon}{4}\sum_{j=0}^{3}\ln^2(1+\gamma_j)\right]+O(\epsilon). \tag{A4}$$

We note that the result (A4) is of the first order in γ_c. This occurs since the terms of the first order in the fluctuation propagator exist in Eq. (A3).

Next, the two-loop contribution to $P_2^{\alpha_1\alpha_2}(i\varepsilon_{n_1},i\varepsilon_{n_2})$ can be written as follows:

$$\big[P_2^{\alpha_1\alpha_2}\big]^{(2)}\big(i\varepsilon_{n_1},i\varepsilon_{n_2}\big)=-\frac{1}{4}\sum_{n_5n_6}\sum_{\beta_1\beta_2}\big\langle\!\big\langle \mathrm{sp}\big[w^{\alpha_1\beta_1}_{n_1n_6}\bar{w}^{\beta_1\alpha_1}_{n_6n_1}\big]\mathrm{sp}\big[\bar{w}^{\alpha_2\beta_2}_{n_2n_5}w^{\beta_2\alpha_2}_{n_5n_2}\big]\big\rangle\!\big\rangle-2\Big\langle \mathrm{sp}\big[w^{\alpha_1\alpha_2}_{n_1n_2}\bar{w}^{\alpha_2\alpha_1}_{n_2n_1}\big]\Big[S^{(4)}_\sigma+S^{(4)}_{\rm int}+\frac{1}{2}\big(S^{(3)}_{\rm int}\big)^2\Big]\Big\rangle. \tag{A5}$$

Here, the term

$$S_\sigma^{(4)} = -\frac{g}{128}\int_{q_j}\delta\left(\sum_{j=0}^{3}\boldsymbol{q_j}\right)\sum_{\beta_1\beta_2\beta_3\beta_4}\sum_{n_5n_6n_7n_8}\mathrm{sp}\big[w_{n_5n_6}^{\beta_1\beta_2}(\boldsymbol{q_0})\bar{w}_{n_6n_7}^{\beta_2\beta_3}(\boldsymbol{q_1})w_{n_7n_8}^{\beta_3\beta_4}(\boldsymbol{q_2})\bar{w}_{n_8n_5}^{\beta_4\beta_1}(\boldsymbol{q_3})\big]$$
$$\times\left[2h^2+\frac{16z}{g}\left(\Omega_{56}^\varepsilon+\Omega_{78}^\varepsilon\right)-(\boldsymbol{q_0}+\boldsymbol{q_1})(\boldsymbol{q_2}+\boldsymbol{q_3})-(\boldsymbol{q_0}+\boldsymbol{q_3})(\boldsymbol{q_1}+\boldsymbol{q_2})\right] \tag{A6}$$

appears in the expansion of S_σ and the regulator term (17) to the fourth order in W. The expansion of the interaction term S_{int} results in the following third- and fourth-order terms:

$$S_{\mathrm{int}}^{(3)} = \frac{\pi T}{4}\sum_{r=0,3}\sum_{j=0}^{3}\Gamma_j\sum_{\alpha,n}\int d\boldsymbol{r}\,\mathrm{Tr}I_n^\alpha t_{rj}W\,\mathrm{Tr}I_{-n}^\alpha t_{rj}\Lambda W^2+\frac{\pi T}{4}\Gamma_c\sum_{\alpha,n}\sum_{r=1,2}\int d\boldsymbol{r}\,\mathrm{Tr}\big[t_{r0}L_n^\alpha W\big]\mathrm{Tr}\big[t_{r0}L_n^\alpha\Lambda W^2\big], \tag{A7}$$

$$S_{\mathrm{int}}^{(4)} = -\frac{\pi T}{16}\sum_{r=0,3}\sum_{j=0}^{3}\Gamma_j\sum_{\alpha,n}\int d\boldsymbol{r}\,\mathrm{Tr}I_n^\alpha t_{rj}\Lambda W^2\,\mathrm{Tr}I_{-n}^\alpha t_{rj}\Lambda W^2-\frac{\pi T}{16}\Gamma_c\sum_{\alpha,n}\sum_{r=1,2}\int d\boldsymbol{r}\big(\mathrm{Tr}\big[t_{r0}L_n^\alpha\Lambda W^2\big]\big)^2. \tag{A8}$$

After evaluation of averages in Eq. (A5), we find

$$\begin{aligned}
\big[P_2^{\alpha_1\alpha_2}\big]^{(2)}(i\varepsilon_{n_1},i\varepsilon_{n_2}) =& -\left(\frac{16}{g}\right)^2\left[\left(\int_q\mathcal{D}_q\big(i\Omega_{12}^\varepsilon\big)\right)^2+\left(\int_q\mathcal{C}_q\big(i\Omega_{12}^\varepsilon\big)\right)^2\right]+\frac{1-9}{4}\left(\frac{16}{g}\right)^2\int_{q,p}\left[p^2+q^2+h^2+\frac{16z}{g}\Omega_{12}^\varepsilon\right]\\
&\times\mathcal{C}_p\big(i\Omega_{12}^\varepsilon\big)\mathcal{D}_q\big(i\Omega_{12}^\varepsilon\big)\big[\mathcal{D}_q\big(i\Omega_{12}^\varepsilon\big)+\mathcal{C}_p\big(i\Omega_{12}^\varepsilon\big)\big]-\left(\frac{64}{g}\right)^2\sum_{j=0}^{3}\frac{\pi T\Gamma_j}{g}\int_{q,p}\left\{\sum_{\omega_n>\varepsilon_{n_1}}+\sum_{\omega_n>-\varepsilon_{n_2}}\right\}\\
&\times\big[\mathcal{D}_p^2\big(i\Omega_{12}^\varepsilon\big)+\mathcal{C}_p^2\big(i\Omega_{12}^\varepsilon\big)\big]\left[p^2+q^2+2h^2+\frac{16Z_\omega}{g}\left(\Omega_{12}^\varepsilon+\omega_n\right)\right]\mathcal{D}_q(i\omega_n)\mathcal{D}_q^{(j)}(i\omega_n)\\
&+\left(\frac{64}{g}\right)^2\sum_{j=0}^{3}\frac{2\pi T\Gamma_j}{g}\int_{q,p}\sum_{\omega_n>0}\left[1-\frac{16\Gamma_j\omega_n}{g}\mathcal{D}_{\boldsymbol{q}+\boldsymbol{p}}^{(j)}(i\omega_n)\right]\\
&\times\big[\mathcal{D}_q^2\big(i\Omega_{12}^\varepsilon\big)\mathcal{D}_p\big(i\Omega_{12}^\varepsilon+i\omega_n\big)+\mathcal{C}_q^2\big(i\Omega_{12}^\varepsilon\big)\mathcal{C}_p\big(i\Omega_{12}^\varepsilon+i\omega_n\big)\big]\\
&-\left(\frac{64}{g}\right)^2\frac{2\pi TZ_\omega}{g}\int_{q,p}\big[\mathcal{D}_p^2\big(i\Omega_{12}^\varepsilon\big)+\mathcal{C}_p^2\big(i\Omega_{12}^\varepsilon\big)\big]\left\{\sum_{\omega_n>\varepsilon_{n_1}}\mathcal{L}_q\big(2i\varepsilon_{n_1}-i\omega_n\big)+\sum_{\omega_n>-\varepsilon_{n_2}}\mathcal{L}_q\big(i\omega_n+2i\varepsilon_{n_2}\big)\right\}\\
&\times\left[p^2+q^2+2h^2+\frac{16Z_\omega}{g}\left(\Omega_{12}^\varepsilon+\omega_n\right)\right]\mathcal{C}_q^2(i\omega_n)+\left(\frac{64}{g}\right)^2\left\{\sum_{j=0}^{3}\frac{\pi T\Gamma_j}{g}\left\{\sum_{\varepsilon_{n_1}>\omega_n\geq 0}+\sum_{-\varepsilon_{n_2}>\omega_n>0}\right\}\right\}\\
&\times\left[1-\frac{16\Gamma_j\omega_n}{g}\mathcal{D}_{\boldsymbol{q}+\boldsymbol{p}}^{(j)}(i\omega_n)\right]\big[\mathcal{D}_q^2\big(i\Omega_{12}^\varepsilon\big)\mathcal{D}_p\big(i\Omega_{12}^\varepsilon-i\omega_n\big)+\mathcal{C}_q^2\big(i\Omega_{12}^\varepsilon\big)\mathcal{C}_p\big(i\Omega_{12}^\varepsilon-i\omega_n\big)\big]\\
&+\frac{2^{13}\pi TZ_\omega}{g^3}\int_{q,p}\left\{\sum_{\omega_n>\varepsilon_{n_1}}\mathcal{L}_{\boldsymbol{q}+\boldsymbol{p}}(i\omega_n-i\mathcal{E}_{12})+\sum_{\omega_n>-\varepsilon_{n_2}}\mathcal{L}_{\boldsymbol{q}+\boldsymbol{p}}(i\omega_n+i\mathcal{E}_{12})\right\}\\
&\times\big[\mathcal{C}_q^2\big(i\Omega_{12}^\varepsilon\big)\mathcal{D}_p(i\omega_n)+\mathcal{D}_q^2\big(i\Omega_{12}^\varepsilon\big)\mathcal{C}_p(i\omega_n)\big].
\end{aligned} \tag{A9}$$

Performing analytic continuation to the real frequencies $i\varepsilon_{n_1}\to E+i0^+$, $i\varepsilon_{n_2}\to E'-i0^+$ in Eq. (A9), we obtain

$$\begin{aligned}
\big[P_2^{\alpha_1\alpha_2}\big]^{RA(2)}(E,E') =& -2\left(\frac{16}{g}\right)^2\left(\int_q\mathcal{D}_q^R(\Omega)\right)^2-\left(\frac{32}{g}\right)^2\int_{q,p}\left[p^2+q^2+h^2-\frac{16Z_\omega}{g}i\Omega\right]\mathcal{D}_p^R(\Omega)\mathcal{D}_q^{R2}(\Omega)\\
&-2\left(\frac{32}{g}\right)^2\sum_{j=0}^{3}\frac{\Gamma_j}{ig}\int_{q,p,\omega}\left[\mathcal{F}_{\omega-E}+\mathcal{F}_{\omega+E'}\right]\left[p^2+q^2+2h^2-\frac{16Z_\omega}{g}i(\Omega+\omega)\right]\mathcal{D}_p^{R2}(\Omega)\mathcal{D}_q^R(\omega)\mathcal{D}_q^{(j)R}(\omega)\\
&-\left(\frac{64}{g}\right)^2\frac{Z_\omega}{ig}\int_{q,p,\omega}\mathcal{C}_p^{R2}(\Omega)\left\{\left[p^2+q^2+2h^2-\frac{16Z_\omega}{g}i(\Omega+2E-\omega)\right]\mathcal{C}_q^{R2}(2E-\omega)\right.\\
&\times\big[\mathcal{L}_q^K(\omega)+\mathcal{F}_{E-\omega}\mathcal{L}_q^R(\omega)\big]+\left[p^2+q^2+2h^2-\frac{16Z_\omega}{g}i(\Omega+\omega-2E')\right]\mathcal{C}_q^{R2}(\omega-2E')
\end{aligned}$$

$$\times\big[\mathcal{L}_q^K(\omega)+\mathcal{F}_{\omega-E'}\mathcal{L}_q^A(\omega)\big]\Big\}+\left(\frac{64}{g}\right)^2\sum_{j=0}^{3}\frac{\Gamma_j}{ig}\int_{q,p,\omega}\mathcal{B}_\omega\left[1+\frac{16\Gamma_j i\omega}{g}\mathcal{D}^{(j)R}_{\boldsymbol{q}+\boldsymbol{p}}(\omega)\right]\mathcal{D}_q^{R2}(\Omega)\mathcal{D}_p^R(\omega+\Omega)$$
$$+\left(\frac{32}{g}\right)^2\sum_{j=0}^{3}\frac{2\Gamma_j}{ig}\int_{q,p,\omega}[2\mathcal{B}_\omega-\mathcal{F}_{\omega-E}-\mathcal{F}_{\omega+E'}]\mathcal{D}_p^R(\Omega-\omega)\mathcal{D}_q^{R2}(\Omega)\left[1+\frac{16\Gamma_j i\omega}{g}\mathcal{D}^{(j)R}_{\boldsymbol{q}+\boldsymbol{p}}(\omega)\right]$$
$$+\left(\frac{64}{g}\right)^2\frac{Z_\omega}{ig}\int_{q,p,\omega}\mathcal{L}^R_{\boldsymbol{q}+\boldsymbol{p}}(\omega)\mathcal{C}_q^{R2}(\Omega)\big\{\mathcal{F}_{\omega-E}\mathcal{C}_p^R(\omega-\mathcal{E})+\mathcal{F}_{\omega+E'}\mathcal{C}_p^R(\omega+\mathcal{E})\big\}\Big]\Big\}. \tag{A10}$$

Here, we again took into account that diffuson $\mathcal{D}_q^R(\omega)$ and cooperon $\mathcal{C}_q^R(\omega)$ propagators are the same. The most part of the two-loop contribution to $[P_2^{\alpha_1\alpha_2}]^{RA}(E,E')$ can be recast in the form of the diffuson and cooperon one-loop contribution renormalized by interaction and disorder (see Appendix B). In the limit $E=E'=T=0$, we arrive (see details for evaluation of the integrals in Ref. [19]) at

$$\big[P_2^{\alpha_1\alpha_2}\big]^{RA(2)}\to -32\frac{t^2h^{2\epsilon}}{\epsilon^2}[3+\epsilon]-16\frac{t^2h^{2\epsilon}}{\epsilon^2}\left[2\sum_{j=0}^{3}f(\gamma_j)+3\sum_{j=0}^{3}\ln(1+\gamma_j)+4\gamma_c\right.$$
$$\left.-\epsilon\sum_{j=0}^{3}\frac{2+\gamma_j}{\gamma_j}\left(\ln(1+\gamma_j)+\mathrm{li}_2(-\gamma_j)+\frac{1}{4}\ln^2(1+\gamma_j)\right)+2\epsilon\gamma_c\right], \tag{A11}$$

where the function $f(x)$ is given by Eq. (31) of the main text and the function $\mathrm{li}_2(x)$ is the polylogarithm. We note that the result (A11) is of the first order in γ_c. This occurs since the terms of the first order in the fluctuation propagator exist in Eq. (A10). Combining Eqs. (A4) and (A11), we arrive at Eq. (29) of the main text.

APPENDIX B: ONE-LOOP RENORMALIZATION OF (MESOSCOPIC) DIFFUSON AND COOPERON PROPAGATORS

In this appendix, we present the one-loop results for the renormalization of the (mesoscopic) diffuson and cooperon propagators. Such renormalization accounts for the significant part of the two-loop contribution to $[P_2^{\alpha_1\alpha_2}]^{RA}(E,E')$. Taking into account Eqs. (26) and (A10), we can rewrite the expression for $[P_2^{\alpha_1\alpha_2}]^{RA}(E,E')$ in the following way:

$$\big[P_2^{\alpha_1\alpha_2}\big]^{RA}(E,E')=-\int_q\frac{256Z(E,E')}{gq^2-16iZ_\omega\Omega-\Sigma^R(q,E,E')}-2\left(\frac{16}{g}\right)^2\left(\int_q\mathcal{D}_q^R(\Omega)\right)^2-4\left(\frac{16}{g}\right)^2\int_{qp}\mathcal{D}_q^{R2}(\Omega). \tag{B1}$$

Here, the renormalization factor $Z(E,E')$ is given as [cf. Eq. (21)]

$$Z(E,E')=1+\frac{16}{ig^2}\sum_{j=0}^{3}\Gamma_j\int_{p,\omega}[\mathcal{F}_{\omega-E}+\mathcal{F}_{\omega+E'}]\mathcal{D}_p^R(\omega)\mathcal{D}_p^{(j)R}(\omega)+\frac{32Z_\omega}{ig^2}\int_{p,\omega}\big\{\mathcal{C}_p^{R2}(2E-\omega)\big[\mathcal{L}_p^K(\omega)+\mathcal{F}_{E-\omega}\mathcal{L}_p^R(\omega)\big]$$
$$+\mathcal{C}_p^{R2}(\omega-2E')\big[\mathcal{L}_p^K(\omega)+\mathcal{F}_{\omega-E'}\mathcal{L}_p^A(\omega)\big]\big\}. \tag{B2}$$

The diffuson self-energy reads as

$$\Sigma^R(q,E,E')=4q^2\int_p\mathcal{D}_p^R(\Omega)-\frac{8}{ig}\sum_{j=0}^{3}\Gamma_j\int_{p,\omega}[2\mathcal{B}_\omega-\mathcal{F}_{\omega-E}-\mathcal{F}_{\omega+E'}]\frac{\mathcal{D}_p^{(j)R}(\omega)}{\mathcal{D}_p^R(\omega)}\big[\mathcal{D}^R_{\boldsymbol{p}+\boldsymbol{q}}(\omega+\Omega)+\mathcal{D}^A_{\boldsymbol{p}-\boldsymbol{q}}(\omega-\Omega)\big]$$
$$+\frac{8}{ig}\sum_{j=0}^{3}\Gamma_j\int_{p,\omega}[\mathcal{F}_{\omega-E}+\mathcal{F}_{\omega+E'}]\mathcal{D}_p^{(j)R}(\omega)\big[2\boldsymbol{pq}\mathcal{D}^R_{\boldsymbol{p}+\boldsymbol{q}}(\omega+\Omega)+\big[\mathcal{D}_q^R(\Omega)\big]^{-1}\big[\mathcal{D}^R_{\boldsymbol{p}+\boldsymbol{q}}(\omega+\Omega)-\mathcal{D}_p^R(\omega)\big]\big]$$
$$-\frac{16Z_\omega}{ig}\big[\mathcal{C}_q^R(\Omega)\big]^{-1}\int_{p,\omega}\big\{\mathcal{C}_p^{R2}(2E-\omega)\big[\mathcal{L}_p^K(\omega)+\mathcal{F}_{E-\omega}\mathcal{L}_p^R(\omega)\big]+\mathcal{C}_p^{R2}(\omega-2E')\big[\mathcal{L}_p^K(\omega)+\mathcal{F}_{\omega-E'}\mathcal{L}_p^A(\omega)\big]\big\}$$
$$-\frac{16Z_\omega}{ig}\int_{p,\omega}\mathcal{L}^R_{\boldsymbol{p}+\boldsymbol{q}}(\omega)\big[\mathcal{F}_{\omega-E}\mathcal{C}_p^R(\omega-\mathcal{E})+\mathcal{F}_{\omega+E'}\mathcal{C}_p^R(\omega+\mathcal{E})\big]$$
$$-\frac{16Z_\omega}{ig}\int_{p,\omega}\big\{\mathcal{C}_p^R(2E-\omega)\big[\mathcal{L}_p^K(\omega)+\mathcal{F}_{E-\omega}\mathcal{L}_p^R(\omega)\big]+\mathcal{C}_p^R(\omega-2E')\big[\mathcal{L}_p^K(\omega)+\mathcal{F}_{\omega-E'}\mathcal{L}_p^A(\omega)\big]\big\}. \tag{B3}$$

Expanding the self-energy $\Sigma^R(q,E,E')$ to the lowest order in ω and q^2, we find

$$\frac{1}{g}\mathcal{D}_q^R(\Omega) \to \frac{Z(E,E)}{g(E)q^2 - i16Z_\omega(E)\Omega + 16Z_\omega(E)\tau_\phi^{-1}(E)}, \tag{B4}$$

where

$$\begin{aligned} g(E) = g &- 4\int_p \mathcal{D}_p^R(0) + \frac{16}{g}\sum_{j=0}^{3}\Gamma_j\int_{p,\omega} p^2[\mathcal{F}_{\omega-E}+\mathcal{F}_{\omega+E}]\mathrm{Im}\big[\mathcal{D}_p^{(j)R}(\omega)\mathcal{D}_p^{R2}(\omega)\big] \\ &+ \frac{64Z_\omega}{g}\int_{p,\omega} p^2\mathcal{F}_{\omega-E}\mathrm{Im}\big[\mathcal{L}_p^R(\omega)\mathcal{C}_p^{R3}(\omega-2E)\big] - \frac{16}{g}\sum_{j=0}^{3}\Gamma_j\int_{p,\omega}[2\mathcal{B}_\omega - \mathcal{F}_{\omega-E}-\mathcal{F}_{\omega+E}] \\ &\times \mathrm{Im}\big[\mathcal{D}_p^{(j)R}(\omega)\big[\mathcal{D}_p^R(\omega)\big]^{-1}\big]\mathrm{Re}\big[\big[1-2p^2\mathcal{D}_p^R(\omega)\big]\mathcal{D}_p^{R2}(\omega)\big] + \frac{64Z_\omega}{g}\int_{p,\omega}[\mathcal{B}_\omega+\mathcal{F}_{E-\omega}]\mathrm{Im}\mathcal{L}_p^R(\omega)\mathrm{Re}\mathcal{C}_p^{R2}(\omega-2E), \end{aligned} \tag{B5}$$

$$\begin{aligned} Z_\omega(E) = Z_\omega &+ \frac{1}{2g}\sum_{j=0}^{3}\Gamma_j\int_{p,\omega}\partial_\omega[\mathcal{F}_{\omega-E}+\mathcal{F}_{\omega+E}]\mathrm{Re}\big[\mathcal{D}_p^{(j)R}(\omega)\big[\mathcal{D}_p^R(\omega)\big]^{-1}\big]\mathrm{Re}\mathcal{D}_p^R(\omega) + \frac{128Z_\omega^2}{g^2}\int_{p,\omega}[\mathcal{B}_\omega+\mathcal{F}_{E-\omega}] \\ &\times \mathrm{Im}\mathcal{L}_p^R(\omega)\mathrm{Re}\mathcal{C}_p^{R2}(\omega-2E) + \frac{4Z_\omega}{g}\int_{p,\omega}\partial_\omega\mathcal{F}_{\omega-E}\mathrm{Re}\big[\mathcal{L}_p^R(\omega)\mathcal{C}_p^R(\omega-2E)\big] \\ &+ \frac{2Z_\omega}{g}\int_{p,\omega}\partial_\omega\mathcal{F}_{\omega-E}\mathrm{Re}\big[\mathcal{L}_p^R(\omega)\mathcal{C}_p^A(\omega-2E)\big] + \frac{4Z_\omega}{g}\int_{p,\omega}\mathcal{F}_{\omega-E}\mathrm{Re}\big[\partial_\omega\mathcal{L}_p^R(\omega)\mathcal{C}_p^R(\omega-2E) - \mathcal{L}_p^R(\omega)\partial_\omega\mathcal{C}_p^R(\omega-2E)\big], \end{aligned} \tag{B6}$$

$$\begin{aligned} \tau_\phi^{-1}(E) = &\frac{4}{g}\sum_{j=0}^{3}\Gamma_j\int_{p,\omega}[2\mathcal{B}_\omega-\mathcal{F}_{\omega-E}-\mathcal{F}_{\omega+E}]\mathrm{Im}\big[\mathcal{D}_p^{(j)R}(\omega)\big[\mathcal{D}_p^R(\omega)\big]^{-1}\big]\mathrm{Re}\mathcal{D}_p^R(\omega) \\ &- \frac{4}{g}\int_{p,\omega}[\mathcal{B}_\omega+\mathcal{F}_{E-\omega}]\mathrm{Im}\mathcal{L}_p^R(\omega)\mathrm{Re}\mathcal{C}_p^R(\omega-2E). \end{aligned} \tag{B7}$$

As one can see, for $|E| \gg T$, the energy $|E|$ indeed serves as the cutoff for the infrared logarithmic divergences in Eqs. (B5) and (B6) (in the case of $L \to \infty$). At the same time, the nonzero value of energy E induces finite dephasing time.

We note that Eqs. (B5) and (B6) reproduce the one-loop renormalization of g and Z_ω, respectively, as it was found in Ref. [16] with the help of the background field method. The Cooper-channel contribution to the dephasing rate [the second line in Eq. (B7)] coincides with the result found in Refs. [58,59].

APPENDIX C: AVERAGE LOCAL DENSITY OF STATES

In this appendix, we present details of a perturbative analysis of the average local density of states. We start from rewriting Eq. (21) in the following form:

$$\langle\rho(E)\rangle = \rho_0 + \delta\rho_{\mathrm{ph}}(E) + \delta\rho_{\mathrm{pp}}^{(1)}(E) + \delta\rho_{\mathrm{pp}}^{(2)}(E), \tag{C1}$$

where

$$\frac{\delta\rho_{\mathrm{ph}}(E)}{\rho_0} = \mathrm{Im}\sum_{j=0}^{3}\frac{16Z_\omega\gamma_j}{g^2}\int_{q,\omega}\mathcal{F}_{\omega-E}\mathcal{D}_q^R(\omega)\mathcal{D}_q^{(j)R}(\omega), \tag{C2}$$

$$\frac{\delta\rho_{\mathrm{pp}}^{(1)}(E)}{\rho_0} = \mathrm{Im}\int_{q,\omega}\frac{32Z_\omega}{g^2}\mathcal{F}_{E-\omega}\mathcal{C}_q^{A2}(\omega-2E)\mathcal{L}_q^A(\omega), \tag{C3}$$

and

$$\begin{aligned} \frac{\delta\rho_{\mathrm{pp}}^{(2)}(E)}{\rho_0} = &\mathrm{Re}\int_{q,\omega}\frac{64Z_\omega}{g^2}\mathcal{C}_q^{R2}(2E-\omega) \\ &\times[\mathcal{B}_\omega+\mathcal{F}_{E-\omega}]\mathrm{Im}\mathcal{L}_q^R(\omega). \end{aligned} \tag{C4}$$

1. Fluctuation corrections above T_c^* at criticality

For temperatures T close to T_c^*, $T - T_c^* \ll T_c^*$, the most important contribution comes from the term $\delta\rho_{\mathrm{pp}}^{(2)}(E)$. In this case, the integrals over frequency and momentum are dominated by region $Dq^2,|\omega| \ll T_c^*$. In this case, the fluctuation propagator (16) can be written in the following form:

$$\mathcal{L}_q^R(\omega) = -\frac{8T_c^*}{\pi}\frac{1}{\tau_{\mathrm{GL}}^{-1}+Dq^2-i\omega}, \tag{C5}$$

where $\tau_{\mathrm{GL}}^{-1} = 8T_c^*|\gamma_c^{-1}(L_T)|/\pi \ll T_c^*$. For energies $|E| \ll T_c^* < T$, taking into account that the RG flow is stopped at

TABLE I. The asymptotic behavior of the scaling function $\mathcal{R}_D(\Omega,Q)$. The scaling of R_D for $|\Omega| \ll 1$ is written in accordance with the Mott's formula. Here, c is a positive constant of the order unity.

	$0 \le |\Omega| \ll 1$	$1 \ll |\Omega|$
$\max\{|\Omega|^{1/d},1\} \ll Q$	(I): $Q^{d-2+\Delta_2}[-i\Omega + c\Omega^2 \ln^{d+1}(1/|\Omega|)]$	(III): $Q^{d-2+\Delta_2}|\Omega|^{-\Delta_2/d}$
$0 \le Q \ll \max\{|\Omega|^{1/d},1\}$	(II): $-i\Omega + c\Omega^2 \ln^{d+1}(1/|\Omega|)$	(IV): $|\Omega|^{(d-2)/d}$

the length scale L_T, we find

$$\frac{\delta\rho_{\rm pp}^{(2)}(E)}{\rho_0} = -t(L_T)(T_c^*\tau_{\rm GL})^{\frac{6-d}{2}}\mathcal{H}_d(2|E|\tau_{\rm GL}). \tag{C6}$$

Here, the function $\mathcal{H}_d(z)$ is given by

$$\mathcal{H}_d(z) = \frac{8}{\pi}\int_0^\infty dy \int_{-\infty}^\infty \frac{dx\, y^{\frac{d-2}{2}}}{(1+y)^2+x^2}\mathrm{Re}\frac{1}{(y+ix-2iz)^2}. \tag{C7}$$

We note that $t(L_T)$ can be approximated by t_* in the critical region $\delta_\xi \ll T_c^*$. Hence, from Eq. (C6) for $|E| \ll \tau_{\rm GL}^{-1}$ we find Eq. (100) with $c_d = \mathcal{H}_d(0)$. We note that $c_2 = 8(1-\ln 2)$ [see Eq. (65)] and $c_3 = 2\pi(3\sqrt{2}-4)$ in agreement with results of Refs. [41–43]. At $|z| \gg 1$, the function $\mathcal{H}_d$ has the following asymptotic behavior: $\mathcal{H}_d(z) \approx -\tilde{c}_d z^{\frac{d-6}{2}}$, where

$$\tilde{c}_d = -\frac{2^{\frac{d}{2}}}{\pi}\int_0^\infty dy \int_{-\infty}^\infty \frac{dx\, y^{\frac{d-2}{2}}}{(1+x)^2+y^2}\mathrm{Re}\frac{y^2-x^2}{(y^2+x^2)^2}. \tag{C8}$$

This asymptote leads to the result given by Eq. (100) for energies $\tau_{\rm GL}^{-1} \ll |E| \ll T_c^*$. We note that $\tilde{c}_3 = \pi/\sqrt{2}$, in agreement with Ref. [43]. We also note that the integral in Eq. (C8) is logarithmically divergent in $d=2$. In this case, one finds $\tilde{c}_2 = 2\ln z$ [see Eq. (66)].

Finally, we consider energies $|E| \gg T_c^*$. The dominant contribution comes from the region $Dq^2, |\omega| \ll T_c^*$ in which the fluctuation propagator can be written in the form (C5). Then, we obtain

$$\frac{\delta\rho_{\rm pp}^{(2)}(E)}{\rho_0} = \frac{4t(L_E)}{\pi}\left(\frac{T_c^*}{E}\right)^2\int_0^{\sim 1} dy \int_0^{\sim 1} \frac{dx\, y^{\frac{d-2}{2}}}{(y+\frac{1}{T_c^*\tau_{\rm GL}})^2+x^2}. \tag{C9}$$

Hence, for $d>2$ the fluctuation correction to the average local density of states at energies $|E| \gg T_c^*$ is proportional to $t(L_E)(T_c^*/E)^2$. In $d=2$, the integral on the right-hand side of Eq. (C9) diverges logarithmically and one obtains Eq. (65).

2. Average local density of states in the insulating phase at $T = 0$

In this section, following the approach proposed in Ref. [18], we evaluate the average LDOS in the insulating phase. In the insulating phase (the region $\delta_\xi \gg T_c^*$ and $t_0 > t_*$), the conductivity can be written in the scaling form

$$g(q,\omega) = \xi^{2-d}\mathcal{R}_D(\omega/\delta_\xi, q\xi). \tag{C10}$$

The asymptotic behavior of the scaling function $\mathcal{R}_D$ is summarized in Table I. Equation (C10) implies the following scaling form for the diffusion coefficient $D = g/16Z_\Omega$:

$$D(q,\omega) = \xi^2(\xi/l)^{-d}E_0\mathcal{R}_D(\omega/\delta_\xi, q\xi). \tag{C11}$$

Here, we have introduced the ultraviolet energy scale $E_0 = 1/(16Z_\omega l^d)$. In what follows, we assume that $t(\xi) \sim t_* \sim 1$ and consider the case of BCS line $\gamma_t = -\gamma_s = \gamma_c = \gamma$. We remind the reader that in the presence of attraction the insulating phase occurs at $\delta_\xi \gg T_c^*$, which implies $|\gamma(\xi)| \ll 1$.

To the lowest order in γ, the contributions of the RG type from the particle-hole and particle-particle channels can be summed and written as

$$\frac{\delta\rho_{\rm ph}(E)+\delta\rho_{\rm pp}^{(1)}(E)}{\rho_0} = 16\Omega_d\mathrm{Im}\int_\varepsilon^\infty d\Omega\int_0^\infty dQ\, Q^{d-1} \times \frac{\gamma(\Omega,Q)}{[R_D(\Omega,Q)Q^2-i\Omega]^2}. \tag{C12}$$

Here, $\gamma(\Omega,Q) = \gamma(\xi)(\max\{Q^{-1},L_\Omega\})^{|\Delta_2|}$ and we have defined $\varepsilon = E/\delta_\xi$. For $|\Omega| \gg 1$, the integral over Q in Eq. (C12) is dominated by $Q \sim |\Omega|^{1/d}$. Then, we obtain

$$\mathrm{Im}\int_0^\infty dQ\, Q^{d-1}\frac{\gamma(\Omega,Q)}{[R_D(\Omega,Q)Q^2-i\Omega]^2} \sim \frac{\gamma(L_\Omega)}{\Omega}. \tag{C13}$$

Hence, we reproduce RG result (113) for $\varepsilon \gg 1$ from Eq. (C12).

For $|\Omega| \ll 1$, the integral over Q in Eq. (C12) is dominated by $Q \sim 1$. Then, we find

$$\mathrm{Im}\int_0^\infty dQ\, Q^{d-1}\frac{\gamma(\Omega,Q)}{[R_D(\Omega,Q)Q^2-i\Omega]^2} \sim \frac{\gamma(\xi)}{\Omega}\ln^{d+1}\frac{1}{|\Omega|}. \tag{C14}$$

Then, integrating over Ω in Eq. (C12), we obtain

$$\frac{\delta\rho_{\rm ph}(E)+\delta\rho_{\rm pp}^{(1)}(E)}{\rho_0} = a_1\gamma(\xi)\ln^{d+2}\frac{1}{|\varepsilon|}, \tag{C15}$$

where a_1 is some positive constant.

The other contribution from the particle-particle channel is of non-RG type. For $|\gamma(\xi)| \ll 1$, this term becomes of the second order in $\gamma(\xi)$:

$$\begin{aligned}\frac{\delta\rho_{\rm pp}^{(2)}(E)}{\rho_0} &= 16\Omega_d\mathrm{Re}\int_0^\varepsilon d\Omega\int_0^\infty \frac{dQ\, Q^{d-1}}{[R_D(\Omega,Q)Q^2-i\Omega]^2} \\ &\quad\times\mathrm{Im}\frac{1}{\gamma^{-1}(\xi)-\ln[R_D(\Omega,Q)Q^2-i\Omega]} \\ &\approx -8\pi\Omega_d\gamma^2(\xi)\mathrm{Re}\int_0^\varepsilon d\Omega \\ &\quad\times\int_0^\infty \frac{dQ\, Q^{d-1}}{[R_D(\Omega,Q)Q^2-i\Omega]^2}.\end{aligned} \tag{C16}$$

For $|\Omega| \gg 1$, the integral over Q in Eq. (C16) is dominated by $Q \sim |\Omega|^{1/d}$:

$$\int_0^\infty \frac{dQ\, Q^{d-1}}{[R_D(\Omega,Q)Q^2-i\Omega]^2} \sim \frac{1}{\Omega}. \tag{C17}$$

Hence, for $\varepsilon \gg 1$ we find

$$\frac{\delta\rho^{(2)}_{\rm pp}(E)}{\rho_0} \sim \gamma^2(\xi)\ln\varepsilon. \tag{C18}$$

This contribution is smaller than the RG result (113).

For $|\Omega| \ll 1$, the integral over Q in Eq. (C16) is dominated by $Q \sim 1$, provided the inequality $d + 2\Delta_2 > 0$ holds. Then, we obtain

$$\frac{\delta\rho^{(2)}_{\rm pp}(E)}{\rho_0} = a_2\gamma^2(\xi){\rm Re}\int_0^\varepsilon \frac{d\Omega}{(\Omega+i0)^2} = -a_2\gamma^2(\xi)\frac{1}{\varepsilon}, \tag{C19}$$

where a_2 stands for a positive constant.

[1] A. M. Goldman and N. Marković, Superconductor-insulator transitions in the two-dimensional limit, Phys. Today **51**, (11) 39 (1998).
[2] V. F. Gantmakher and V. T. Dolgopolov, Superconductor-insulator quantum phase transition, Phys.-Usp. **53**, 1 (2010).
[3] B. Sacépé, C. Chapelier, T. I. Baturina, V. M. Vinokur, M. R. Baklanov, and M. Sanquer, Disorder-Induced Inhomogeneities of the Superconducting State Close to the Superconductor-Insulator Transition, Phys. Rev. Lett. **101**, 157006 (2008).
[4] B. Sacépé, C. Chapelier, T. I. Baturina, V. M. Vinokur, M. R. Baklanov, and M. Sanquer, Pseudogap in a thin film of a conventional superconductor, Nat. Commun. **1**, 140 (2010).
[5] B. Sacépé, Th. Dubouchet, C. Chapelier, M. Sanquer, M. Ovadia, D. Shahar, M. Feigel'man, and L. Ioffe, Localization of preformed Cooper pairs in disordered superconductors, Nat. Phys. **7**, 239 (2011).
[6] D. Sherman, B. Gorshunov, S. Poran, N. Trivedi, E. Farber, M. Dressel, and A. Frydman, Effect of Coulomb interactions on the disorder-driven superconductor-insulator transition, Phys. Rev. B **89**, 035149 (2014).
[7] M. Mondal, A. Kamlapure, M. Chand, G. Saraswat, S. Kumar, J. Jesudasan, L. Benfatto, V. Tripathi, and P. Raychaudhuri, Phase Fluctuations in a Strongly Disordered s-Wave NbN Superconductor Close to the Metal-Insulator Transition, Phys. Rev. Lett. **106**, 047001 (2011).
[8] Y. Noat, V. Cherkez, C. Brun, T. Cren, C. Carbillet, F. Debontridder, K. Ilin, M. Siegel, A. Semenov, H.-W. Hübers, and D. Roditchev, Unconventional superconductivity in ultrathin superconducting NbN films studied by scanning tunneling spectroscopy, Phys. Rev. B **88**, 014503 (2013).
[9] P. Szabò, T. Samuely, V. Haškovà, J. Kačmarčìk, M. Žemlička, M. Grajcar, J. G. Rodrigo, and P. Samuely, Fermionic scenario for the destruction of superconductivity in ultrathin MoC films evidenced by STM measurements, Phys. Rev. B **93**, 014505 (2016).
[10] A. Ghosal, M. Randeria, and N. Trivedi, Role of Spatial Amplitude Fluctuations in Highly Disordered s-Wave Superconductors, Phys. Rev. Lett. **81**, 3940 (1998).
[11] A. Ghosal, M. Randeria, and N. Trivedi, Inhomogeneous pairing in highly disordered s-wave superconductors, Phys. Rev. B **65**, 014501 (2001).
[12] K. Bouadim, Y. L. Loh, M. Randeria, and N. Trivedi, Single- and two-particle energy gaps across the disorder-driven superconductor-insulator transition, Nat. Phys. **7**, 884 (2011).
[13] M. V. Feigel'man, L. B. Ioffe, V. E. Kravtsov, and E. A. Yuzbashyan, Eigenfunction Fractality and Pseudogap State Near the Superconductor-Insulator Transition, Phys. Rev. Lett. **98**, 027001 (2007).
[14] M. V. Feigel'man, L. B. Ioffe, V. E. Kravtsov, and E. Cuevas, Fractal superconductivity near localization threshold, Ann. Phys. (N.Y.) **325**, 1390 (2010).
[15] I. S. Burmistrov, I. V. Gornyi, and A. D. Mirlin, Enhancement of the Critical Temperature of Superconductors by Anderson Localization, Phys. Rev. Lett. **108**, 017002 (2012).
[16] I. S. Burmistrov, I. V. Gornyi, and A. D. Mirlin, Superconductor-insulator transitions: phase diagram and magnetoresistance, Phys. Rev. B **92**, 014506 (2015).
[17] I. S. Burmistrov, I. V. Gornyi, and A. D. Mirlin, Multifractality at Anderson Transitions with Coulomb Interaction, Phys. Rev. Lett. **111**, 066601 (2013).
[18] I. S. Burmistrov, I. V. Gornyi, and A. D. Mirlin, Tunneling into the localized phase near Anderson transitions with Coulomb interaction, Phys. Rev. B **89**, 035430 (2014).
[19] I. S. Burmistrov, I. V. Gornyi, and A. D. Mirlin, Multifractality and electron-electron interaction at Anderson transitions, Phys. Rev. B **91**, 085427 (2015).
[20] F. Wegner, The mobility edge problem: Continuous symmetry and a conjecture, Z. Phys. B: Condens. Matter **35**, 207 (1979).
[21] K. B. Efetov, A. I. Larkin, and D. E. Khmelnitskii, Interaction of diffusion modes in the theory of localization, Zh. Eksp. Teor. Fiz. **79**, 1120 (1980) [Sov. Phys.–JETP **52**, 568 (1980)].
[22] A. M. Finkel'stein, The influence of Coulomb interaction on the properties of disordered metals, Zh. Eksp. Teor. Fiz. **84**, 168 (1983) [Sov. Phys.–JETP **57**, 97 (1983)].
[23] A. M. Finkel'stein, Weak-localization and Coulomb interactions in disordered systems, Z. Phys. B: Condens. Matter **56**, 189 (1984).
[24] A. M. Finkel'stein, *Electron Liquid in Disordered Conductors*, edited by I. M. Khalatnikov, Soviet Scientific Reviews, Vol. 14 (Harwood Academic, Reading, UK, 1990).
[25] D. Belitz and T. R. Kirkpatrick, The Anderson-Mott transition, Rev. Mod. Phys. **66**, 261 (1994).
[26] A. M. M. Pruisken, M. A. Baranov, and B. Škorić, (Mis-)handling gauge invariance in the theory of the quantum hall effect. I. Unifying action and the $\nu = 1/2$ state, Phys. Rev. B **60**, 16807 (1999).
[27] B. L. Al'tshuler and A. G. Aronov, *Electron-electron Interactions in Disordered Conductors* (Elsevier, North-Holland, 1985).
[28] A. Kamenev and A. Levchenko, Keldysh technique and non-linear σ-model: basic principles and applications, Adv. Phys. **58**, 197 (2009).
[29] C. Castellani, C. Di Castro, P. A. Lee, and M. Ma, Interaction-driven metal-insulator transitions in disordered fermion systems, Phys. Rev. B **30**, 527 (1984).
[30] D. J. Amit, *Field Theory, the Renormalization Group, and Critical Phenomena* (World Scientific, Singapore, 1993).

[31] B. L. Al'tshuler and A. G. Aronov, Zero bias anomaly in tunnel resistance and electron-electron interaction, Solid State Commun. **30**, 115 (1979).

[32] M. A. Baranov, A. M. M. Pruisken, and B. Škorić, (Mis-) handling gauge invariance in the theory of the quantum hall effect. II. Perturbative results, Phys. Rev. B **60**, 16821 (1999).

[33] B. L. Al'tshuler and A. G. Aronov, Contribution to the theory of disordered metals in strongly doped semiconductors, Zh. Eksp. Teor. Fiz. **77**, 2028 (1979) [Sov. Phys.–JETP **50**, 968 (1979)].

[34] B. L. Al'tshuler, A. G. Aronov, and P. A. Lee, Interaction Effects in Disordered Fermi Systems in Two Dimensions, Phys. Rev. Lett. **44**, 1288 (1980).

[35] D. Höf and F. Wegner, Calculation of anomalous dimensions for the nonlinear sigma model, Nucl. Phys. B **275**, 561 (1986).

[36] F. Wegner, Anomalous dimesions for the nonlinear sigma-model in $2+\epsilon$ dimensions (I), Nucl. Phys. B **280**, 193 (1987).

[37] F. Wegner, Anomalous dimensions for the nonlinear sigma-model, in $2+\epsilon$ dimensions (II), Nucl. Phys. B **280**, 210 (1987).

[38] B. L. Altshuler, V. E. Kravtsov, and I. V. Lerner, *Distribution of Mesoscopic Fluctuations and Relaxation Processes in Disordered Conductors*, edited by B. L. Altshuler, P. A. Lee, and R. A. Webb, Mesoscopic Phenomena in Solids, Vol. 449 (North-Holland, Amsterdam, 1991).

[39] A. D. Mirlin, Statistics of energy levels and eigenfunctions in disordered systems, Phys. Rep. **326**, 259 (2000).

[40] E. J. König, A. Levchenko, I. V. Protopopov, I. V. Gornyi, I. S. Burmistrov, and A. D. Mirlin, Berezinskii-Kosterlitz-Thouless transition in homogeneously disordered superconducting films, Phys. Rev. B **92**, 214503 (2015).

[41] E. Abrahams, M. Redi, and J. W. F. Woo, Effect of fluctuations on electronic properties above the superconducting transition, Phys. Rev. B **1**, 208 (1970).

[42] J. P. Hurault and K. Maki, Breakdown of the mean field theory in the superconducting transition region, Phys. Rev. B **2**, 2560 (1970).

[43] C. Di Castro, R. Raimondi, C. Castellani, and A. A. Varlamov, Superconductive fluctuations in the density of states and tunneling resistance in high-T_c superconductors, Phys. Rev. B **42**, 10211 (1990).

[44] A. I. Larkin and Yu. N. Ovchinnikov, Nonlinear fluctuation phenomena in the transport properties of superconductors, JETP **92**, 519 (2001).

[45] A. Levchenko, Transport theory of superconductors with singular interaction corrections, Phys. Rev. B **81**, 012507 (2010).

[46] To make the plots we change $1-8(1-\ln 2)t_c(T_c\tau_{\rm GL})^2$ in Eq. (65) to $1/[1+8(1-\ln 2)t_c(T_c\tau_{\rm GL})^2]$.

[47] C. Castellani, C. Di Castro, G. Forgacs, and S. Sorella, Spin orbit coupling in disordered interacting electron gas, Solid State Commun. **52**, 261 (1984).

[48] M. Ma and E. Fradkin, Superconductivity and Localization in the Presence of Strong Spin-Orbit Scattering, Phys. Rev. Lett. **56**, 1416 (1986).

[49] A. M. Finkel'stein, Superconducting transition temperature in amorphous films, Pisma Zh. Eksp. Teor. Fiz. **45**, 37 (1987) [JETP Lett. **45**, 46 (1987)].

[50] Yu. V. Nazarov, Anomalous current-voltage characteristics of tunnel junctions, Zh. Eksp. Teor. Fiz. **95**, 975 (1979) [Sov. Phys.–JETP **68**, 561 (1989)].

[51] L. S. Levitov and A. V. Shytov, Semiclassical theory of the Coulomb anomaly, Pisma Zh. Eksp. Teor. Fiz. **66**, 200 (1997) [JETP Lett. **66**, 214 (1997)].

[52] M. A. Skvortsov and M. V. Feigel'man, Superconductivity in Disordered Thin Films: Giant Mesoscopic Fluctuations, Phys. Rev. Lett. **95**, 057002 (2005).

[53] A. Mildenberger, F. Evers, and A. D. Mirlin, Dimensionality dependence of the wave-function statistics at the Anderson transition, Phys. Rev. B **66**, 033109 (2002).

[54] I. S. Burmistrov, S. Bera, F. Evers, I. V. Gornyi, and A. D. Mirlin, Wave function multifractality and dephasing at metal-insulator and quantum Hall transitions, Ann. Phys. (N.Y.) **326**, 1457 (2011).

[55] K. Slevin and T. Ohtsuki, Corrections to Scaling at the Anderson Transition, Phys. Rev. Lett. **82**, 382 (1999).

[56] K. Slevin and T. Ohtsuki, Critical exponent for the Anderson transition in the three-dimensional orthogonal universality class, New J. Phys. **16**, 015012 (2014).

[57] The authors of Ref. [9] observed neither a depletion of LDOS around zero energy above T_c nor sizable spatial fluctuations of LDOS in MoC films. This can be presumably attributed to the fact that all the measurements in Ref. [9] were carried out quite far from SIT (on its superconducting side). Indeed, the largest value of the resistance maximum (t_c) in this work was 1.4kΩ, i.e., 20 times lower than the quantum value h/e^2. We expect that if measurement would be conducted on more resistive samples (closer to the SIT as well as on the insulating side of SIT), all the effects analyzed in our paper (and observed in TiN, InO, and NbN films) would emerge.

[58] W. Brenig, M. C. Chang, E. Abrahams, and P. Wölfle, Inelastic scattering time above the superconductivity transition in two dimensions: Dependence on disorder and magnetic field, Phys. Rev. B **31**, 7001 (1985).

[59] M. Yu. Reizer, Fluctuation conductivity above the superconducting transition: Regularization of the Maki-Thompson term, Phys. Rev. B **45**, 12949 (1992).